

Toward Ultra-Long-Horizon Sequential Model Editing

Mingda Liu ^{*1} Zhenghan Zhu ^{*1} Ze'an Miao ^{*1} Katsuki Fujisawa ¹

Abstract

Model editing has emerged as a practical approach for mitigating factual errors and outdated knowledge in large language models (LLMs). Among existing methods, the Locate-and-Edit (L&E) paradigm is the dominant framework: it locates MLP parameters implicated in expressing a target fact, and then performs a localized update to rewrite that fact. However, long sequences of edits often trigger abrupt model collapse in L&E beyond a critical point. We empirically identify a strong correlation between collapse and explosive growth of edited MLP weight norms, and formally prove that commonly used L&E update rules can induce exponential norm growth across sequential edits in the absence of explicit norm control. To address this issue, we propose Norm-Anchor Scaling (NAS), a plug-and-play norm-constrained strategy. Across extensive experiments, NAS delays the collapse point of representative L&E algorithms by more than $4\times$ and yields a **72.2%** average relative gain in editing performance, requiring only a **single additional line of code** and incurring **negligible computational overhead**. Code is publicly available at <https://github.com/SasyaTitech/NAS>.

1. Introduction

Large language models (LLMs) can store and retrieve substantial amounts of factual knowledge during inference (Petroni et al., 2019; Roberts et al., 2020), yet they still frequently produce hallucinations, factual errors, and outdated information in real-world use (Lin et al., 2022; De Cao et al., 2021; Dhingra et al., 2022). Retraining from scratch to correct such issues is prohibitively expensive (De Cao et al., 2021); meanwhile, conventional fine-tuning over a large parameter subset is more practical but often fails to achieve precise, localized corrections and may introduce

^{*}Equal contribution ¹Institute of Science Tokyo. Correspondence to: Katsuki Fujisawa <fujisawa.k.2110@m.isct.ac.jp>, Mingda Liu <puppetsasya@gmail.com>.

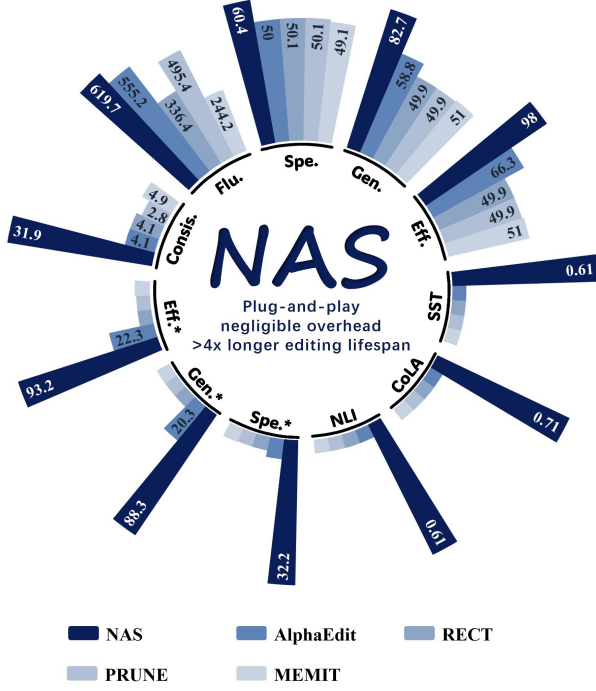


Figure 1. Overview of *ultra-long* sequential knowledge editing performance on LLaMA3 under the Locate-and-Edit (L&E) paradigm, evaluated on the **full** CounterFact stream (**20,877** edits) and ZsRE stream (**19,082** edits). Metrics marked with an asterisk (*) correspond to ZsRE; all others are from CounterFact. See Section 4.2 for the complete setup and detailed results.

hard-to-predict global side effects (Zhang & Wu, 2024). This motivates **knowledge editing**, which aims to update a small portion of model parameters—without full retraining—so that the model reliably outputs the desired new fact under the corresponding prompts (De Cao et al., 2021; Mitchell et al., 2021).

Among knowledge editing paradigms, **Locate-then-Edit (L&E)**(Meng et al., 2023a;b) has been widely adopted. I.e. methods first locate a relevant MLP layer ℓ , then apply a localized low-rank update to its matrix $W^{(\ell)}$ to enforce the new fact. L&E methods are popular largely because they are computationally efficient and tend to produce more “local” modifications, thereby reducing disruption to the model’s overall behavior(Wang et al., 2024b; Yao et al., 2023).

However, a key obstacle to making knowledge editing a

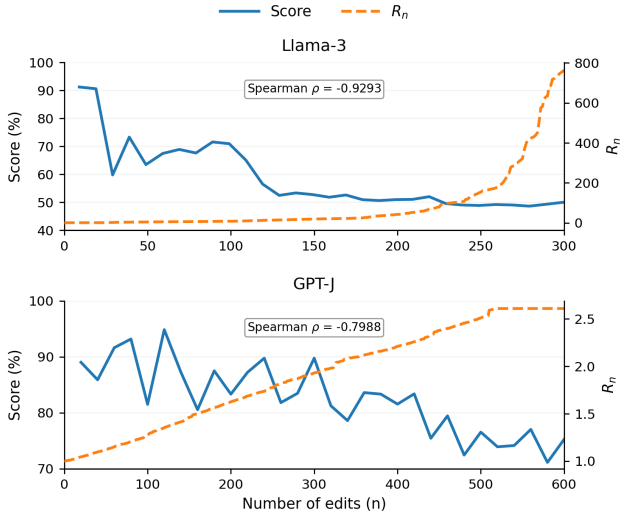


Figure 2. Norm explosion accompanies sequential editing collapse. During sequential vanilla locate-and-edit, we track edit success (blue, left axis) and normalized weight growth $R_n := \|W_n\|/\|W_0\|$ (orange, right axis) versus edit step n . For both Llama-3 and GPT-J, increasing R_n coincides with deteriorating editing performance; Spearman ρ is shown in each panel.

practical lifelong knowledge updating mechanism is *sequential editing*(Gupta et al., 2024b): the model must process a long stream of edit requests within the same parameter space. Prior studies and practice commonly observe that as the number of edits grows, many methods gradually degrade(Meng et al., 2023b; Zhang et al., 2025): editing performance drops, generalization and specificity worsen, side effects accumulate, and general capabilities can substantially decline. While recent work explores more elaborate objectives or statistical constraints to extend the editable horizon(Fang et al., 2024; Ma et al., 2024), long-horizon stability remains a major bottleneck for L&E in practice.

This paper first reports a recurring phenomenon across diverse L&E settings(Gupta et al., 2024a; Xu et al., 2025; Gupta et al., 2025): performance degradation often *co-occurs* with persistent growth in the norm of the target matrix. In Fig. 2, we visualize the joint evolution of editing performance and $\|W_n\|$ ’s normalized measure R_n , using a dual-axis plot, and quantify the trend via Spearman correlation. Motivated by this observation, we go beyond empirical correlation and, to our knowledge, **provide the first mechanistic formalization of norm blow-up in mainstream L&E methods**, together with an explicit analytical derivation of its exponential growth behavior. Empirically, $\log R_n$ is approximately linear in the edit step n , yielding strong exponential fits that match the analytically derived growth pattern.

This is consistent with a stability view: uncontrolled growth in $\|W^{(\ell)}\|$ increases the scale of the edited pathway, poten-

tially making the model more sensitive under off-target contexts and amplifying unintended responses (Scaman & Virmaux, 2019). Moreover, excessive magnitude can push Transformer computations into numerically unfavorable regimes—e.g., overly large $q^\top k$ scores make softmax attention prone to saturation (Henry et al., 2020)—and in LLM training, such scale blow-ups have been linked to sudden gradient-norm growth and loss spikes, suggesting that subsequent optimization steps can become increasingly brittle without explicit scale control (Takase et al., 2025; Xiong et al., 2020).

Based on these insights, we propose *Norm-Anchor Scaling* (NAS), a plug-and-play “norm anchoring” stabilizer for the L&E paradigm. NAS rescales each edit write vector/update to an anchor magnitude estimated from the *unedited* base model—a stable reference scale measured on clean activations—while preserving the update direction. By preventing abnormal magnitude inflation, NAS keeps the write signal within a numerically stable operating range for long-horizon sequential updates. We formally prove that under NAS, the target-layer weight norm admits a finite theoretical upper bound over long edit sequences. Empirically, compared to vanilla L&E updates, NAS confines the target-layer norm drift to a much tighter band around its pre-edit value (Fig. 6), and substantially suppresses the drift of hidden representations(Fig. 4).

NAS is a **one-line drop-in with negligible computational overhead** (Appendix C.6). Extensive experiments show that NAS significantly delays the degradation point (by more than $4\times$ on average) and improves sequential editing performance: the average editing success increases from **51.9 to 89.3 (+37.4 percentage points; +72.2% relative)**. Under our long-horizon *atomic sequential editing* (one request per step) on the full ZsRE (**19,086** edits) and CounterFact (**20,877** edits) streams, NAS is the *only* approach among our evaluated baselines that does not exhibit a clear degradation.

2. Preliminaries

2.1. Knowledge Editing Setup

Factual knowledge in LLMs is often described as a triple (s, r, o) (subject, relation, object), which can be queried by a prompt $x = \text{Prompt}(s, r)$ such that the model should generate o . A knowledge editing request specifies a target object o^* for the same prompt x , and aims to modify a localized set of parameters so that the edited model assigns high probability to o^* under x while preserving unrelated behaviors.

2.2. Transformer FFN as Key–Value Memory

We focus on the FFN module at a fixed layer l . Following the key–value interpretation of FFNs (Geva et al., 2021),

we view the intermediate activation as a *key* k that matches factual patterns, while the FFN output is a retrieved *value* v that encodes the information to be written into the hidden state. let $W_{\text{out}}^{(l)}$ denote the FFN output projection; then

$$v = W_{\text{out}}^{(l)} k. \quad (1)$$

For simplicity, we write $W := W_{\text{out}}^{(l)}$ henceforth.

2.3. Locate-and-Edit Paradigm

Locate-and-Edit (L&E) methods update a localized FFN matrix W to rewrite a specific factual association. After selecting an editing site, we obtain a key vector k^* that represents the query (e.g., the pair (s, r)) at that site. The pre-edit value is

$$v^{\text{old}} := W k^*. \quad (2)$$

Overall update objective. The core objective is to modify W so that the target key k^* maps to a desired value v^{new} , while keeping the original input–output behavior of W on typical keys as unchanged as possible:

$$\begin{aligned} \min_{W'} \mathbb{E}_{k \sim \mathcal{D}} \|W' k - W k\|^2 \\ \text{s.t. } W' k^* = v^{\text{new}}, \end{aligned} \quad (3)$$

where \mathcal{D} denotes a text-induced distribution over FFN keys.

Closed-form rank-one update of W . let $C := \mathbb{E}_{k \sim \mathcal{D}}[k k^\top]$ be the (pre-computed) second-moment matrix of keys. Following prior L&E methods, the constrained problem (3) admits a closed-form rank-one solution (Meng et al., 2023a). Define the per-edit update ΔW as

$$\Delta W := (v^{\text{new}} - v^{\text{old}}) \frac{(C^{-1} k^*)^\top}{(k^*)^\top C^{-1} k^*}. \quad (4)$$

Then the updated matrix is

$$W' = W + \Delta W, \quad (5)$$

which enforces $W' k^* = v^{\text{new}}$ while minimizing the expected disturbance $\mathbb{E}_{k \sim \mathcal{D}} \|W' k - W k\|^2$.

Computing the target value v^{new} . The target value for the new fact is obtained by optimizing an additive correction $\Delta \in \mathbb{R}^d$ under the edit prompt $x = \text{Prompt}(s, r)$:

$$\Delta \in \arg \min_{\Delta \in \mathbb{R}^d} \mathcal{L}_{\text{NLL}}(o^* | x; v^{\text{old}} + \Delta), \quad (6)$$

where \mathcal{L}_{NLL} is evaluated with the FFN output at the editing site replaced by $v^{\text{old}} + \Delta$. The target value is then defined as

$$v^{\text{new}} := v^{\text{old}} + \Delta. \quad (7)$$

2.4. Sequential Editing

Sequential editing applies a stream of requests $\{(s_n, r_n, o_n^*)\}_{n=1}^T$ to the same base model. Focusing on the edited matrix W , the parameter trajectory follows

$$\begin{aligned} W_0 &= W_{\text{base}}, \\ W_n &= W_{n-1} + \Delta W_n, \quad n = 1, \dots, T. \end{aligned} \quad (8)$$

For the n -th request, the pre-edit value is given by

$$v_n^{\text{old}} = W_{n-1} k_n^*. \quad (9)$$

and the closed-form per-edit update is

$$\Delta W_n := (v_n^{\text{new}} - v_n^{\text{old}}) \frac{(C^{-1} k_n^*)^\top}{(k_n^*)^\top C^{-1} k_n^*}. \quad (10)$$

In the next section, we analyze the induced dynamics of $\|W_n\|^2$ and relate them to the norm statistics of v_n^{old} and v_n^{new} .

3. Analysis and Method

3.1. Computing $\|W_n\|^2$

In this section, we conduct both the analysis and all sequential-editing experiments under the Euclidean metric. We focus on the most basic locate-and-edit (L&E) update without additional statistical constraints, and thus set $C = I$ for clarity. Under this setting, The general $C \neq I$ case follows with an analogy; see Appendix B.5. Under this setting, Eq. (10) becomes:

$$\Delta W_n = \frac{(v_n^{\text{new}} - v_n^{\text{old}}) k_n^{*\top}}{\|k_n^*\|^2}. \quad (11)$$

Combining Eqs. (8) and (11) yields an explicit recursion for $\|W_n\|^2$.

lemma 3.1. *The squared norm of the edited weight matrix satisfies*

$$\|W_n\|^2 = \|W_{n-1}\|^2 + \frac{\|v_n^{\text{new}}\|^2 - \|v_n^{\text{old}}\|^2}{\|k_n^*\|^2}. \quad (12)$$

The proof is deferred to Appendix B.2.

Exponential growth of $\|W_n\|^2$. Taking expectation on both sides of Eq. (12) yields the following consequence.

Proposition 3.2. *There exist constants $\alpha \in \mathbb{R}, R > 1$ such that*

$$\mathbb{E} \|W_n\|^2 \approx R^n \mathbb{E} \|W_0\|^2 + \alpha (R^n - 1). \quad (13)$$

Consequently, $\mathbb{E} \|W_n\|^2$ grows exponentially with the number of edits.

The proof is deferred to Appendix B.3.

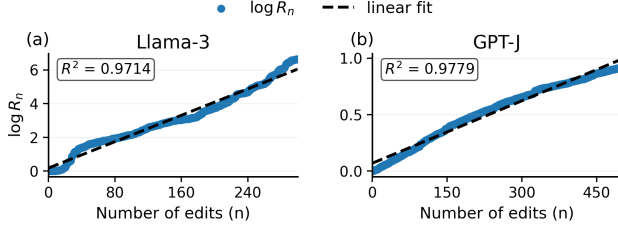


Figure 3. Log-linear growth of weight-norm ratio under sequential editing. We measure $\log R_n$ as a function of edit step n ($R_n = \|W_n\|/\|W_0\|$) for Llama-3 and GPT-J. Linear fits (dashed) achieve high R^2 , supporting an approximately exponential increase of $\|W_0\|$ with the number of edits.

Verification via curve fitting. We fit $\|W_n\|$ as a function of n and observe a clear exponential trend (Fig. 3). In particular, a linear fit on $\log(\cdot)$ -scaled trajectories corroborates the predicted exponential growth.

3.2. Method

Motivation. Section 3.1 suggests that under unconstrained locate-and-edit (L&E) updates, the edited weight norm can grow rapidly with the number of edits. Empirically, $\|v_n^{\text{new}}\|^2$ increases with the current state (e.g., $\|W_{n-1}\|^2$; Fig. 9), forming a positive feedback loop: larger $\|W\|^2$ induces larger target values, which in turn further amplify $\|W\|^2$ through the rank-one updates.

Norm anchoring via rescaling. We break this feedback by explicitly controlling the magnitude of the injected value vector. let

$$a := \mathbb{E}\|v_n^{\text{new}}\|^2; \text{ measured on a clean (unedited) model,} \quad (14)$$

where the expectation is estimated by performing pilot edits on N randomly sampled facts and averaging the resulting $\|v_n^{\text{new}}\|^2$ (Implementation details and ablation of N in Appendix A.3).

For each edit step n , suppose the base editor produces an unconstrained target value \hat{v}_n^{new} . We then rescale it as

$$v_n^{\text{new}} \leftarrow \hat{v}_n^{\text{new}} \cdot \sqrt{\frac{a}{\|\hat{v}_n^{\text{new}}\|^2}}, \quad (15)$$

which enforces $\|v_n^{\text{new}}\|^2 = a$ by construction. Intuitively, this introduces negative feedback: as the system drifts and the unconstrained $\|\hat{v}_n^{\text{new}}\|^2$ grows, the rescaling factor shrinks accordingly.

Implication for weight-norm dynamics. We next show that norm anchoring removes the divergence predicted by the unconstrained analysis.

Corollary 3.3. *If we implement Eq. 15 for each $n \in \{1, 2, \dots, T\}$, then there exist constants $\beta > 0$, $r \in (0, 1)$*

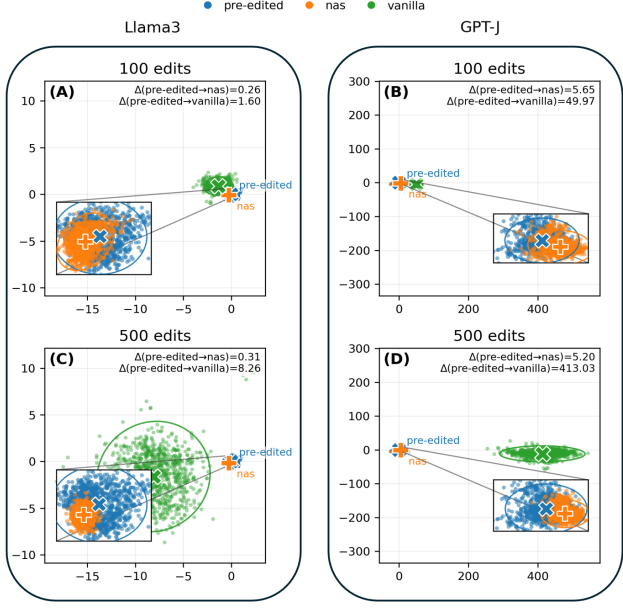


Figure 4. Hidden representation drift under sequential L&E updates. We probe the target-module representations on 1,000 held-out factual prompts for *pre-edited* (blue), *vanilla* (green), and *vanilla+NAS* (orange) after 100 and 500 edits, and visualize them in a shared 2D PCA space (PCA fit on *pre-edited*). Cross markers indicate state-wise means; ellipses denote 95% confidence regions. We report $\Delta(\text{pre} \rightarrow \cdot) = \|\mu_{\cdot} - \mu_{\text{pre}}\|_2$ (centroid distance in the original hidden space).

such that

$$\mathbb{E}\|W_n\|^2 \approx r^n \mathbb{E}\|W_0\|^2 + \beta(1 - r^n). \quad (16)$$

Consequently, $\mathbb{E}\|W_n\|^2$ remains bounded as $n \rightarrow \infty$.

The proof is deferred to Appendix B.4.

Hidden representation drift. To probe activation stability under long sequential updates, we sample target-layer representations on 1,000 *held-out* factual prompts that are disjoint from the edit stream, from three model states: *pre-edited*, *vanilla* L&E, and *vanilla+NAS*. At 100 and 500 cumulative edits, we project representations into a shared 2D PCA space. Figure 4 shows a clear failure mode of *vanilla* L&E: as edits accumulate, representations exhibit a substantial centroid shift and markedly increased dispersion relative to the *pre-edited* distribution, and the drift amplifies sharply from 100 to 500 edits. In contrast, *NAS*-stabilized updates keep the representation cloud tightly aligned with the *pre-edited* distribution. This observation suggests that sequential degradation is accompanied by an out-of-distribution (OOD) shift in target-layer activations, which can cause downstream layers to operate outside their pre-training regime and thereby trigger broad behavioral failures. We next quantify these effects under long-horizon sequential editing in Section 4.

Table 1. RQ1: Long-Horizon sequential model editing results. For each model: Pre-edited is separated by a rule; Non-LE baselines appear above the next rule; LE-family methods appear below. Best in **bold**, second-best in underlined.

Model	Method	Counterfact					ZsRE		
		Eff.↑	Gen.↑	Spe.↑	Flu.↑	Consis.↑	Eff.↑	Gen.↑	Spe.↑
LLaMA3	Pre-edited	7.18 \pm 0.13	9.39 \pm 0.09	89.79 \pm 0.21	568.53 \pm 1.11	3.55 \pm 0.04	36.11 \pm 0.24	35.06 \pm 0.37	32.09 \pm 0.30
	FT	<u>68.69\pm0.30</u>	<u>61.99\pm0.21</u>	40.91 \pm 0.38	325.90 \pm 0.41	1.44 \pm 0.05	8.58 \pm 0.04	6.96 \pm 0.05	17.30 \pm 0.23
	UltraEdit	60.06 \pm 0.20	52.90 \pm 0.18	43.88 \pm 0.14	558.79 \pm 0.70	11.70 \pm 0.34	<u>77.61\pm0.13</u>	75.15 \pm 0.33	50.26\pm0.13
	RLEdit	65.38 \pm 0.29	49.18 \pm 0.26	47.86 \pm 0.30	<u>596.19\pm0.11</u>	<u>12.18\pm0.33</u>	<u>81.59\pm0.35</u>	<u>78.77\pm0.17</u>	27.03 \pm 0.35
	MEMIT	50.95 \pm 0.14	50.95 \pm 0.19	49.05 \pm 0.23	244.21 \pm 0.29	4.86 \pm 0.13	0.95 \pm 0.03	0.22 \pm 0.06	0.22 \pm 0.06
	PRUNE	49.88 \pm 0.21	49.87 \pm 0.13	<u>50.13\pm0.27</u>	495.37 \pm 0.18	2.77 \pm 0.11	0.00 \pm 0.00	0.00 \pm 0.00	0.00 \pm 0.00
	RECT	49.91 \pm 0.15	49.91 \pm 0.38	50.09 \pm 0.28	336.42 \pm 0.24	4.07 \pm 0.09	0.00 \pm 0.00	0.00 \pm 0.00	0.00 \pm 0.00
	AlphaEdit	66.27 \pm 0.34	58.75 \pm 0.20	49.98 \pm 0.17	555.21 \pm 1.06	4.12 \pm 0.12	22.30 \pm 0.32	20.34 \pm 0.15	1.57 \pm 0.03
	NAS	97.95\pm0.32	82.71\pm0.19	60.44\pm0.23	619.72\pm0.41	31.88\pm0.32	93.17\pm0.35	88.30\pm0.33	32.15 \pm 0.13
	Pre-edited	12.58 \pm 0.17	15.26 \pm 0.25	86.24 \pm 0.28	338.63 \pm 0.28	6.87 \pm 0.09	34.83 \pm 0.14	33.76 \pm 0.16	38.60 \pm 0.20
Qwen2.5	FT	<u>88.45\pm0.14</u>	69.30\pm0.26	42.18 \pm 0.13	532.51 \pm 0.20	2.70 \pm 0.03	21.15 \pm 0.35	10.23 \pm 0.19	3.42 \pm 0.10
	UltraEdit	63.03 \pm 0.21	55.78 \pm 0.23	40.34 \pm 0.33	575.56 \pm 0.27	18.33 \pm 0.17	65.76 \pm 0.19	62.81 \pm 0.23	28.19 \pm 0.17
	RLEdit	75.50 \pm 0.27	53.83 \pm 0.36	46.09 \pm 0.16	605.33 \pm 0.25	14.29 \pm 0.35	93.75 \pm 0.33	85.37 \pm 0.20	35.61 \pm 0.20
	MEMIT	51.27 \pm 0.25	51.28 \pm 0.10	48.73 \pm 0.14	524.64 \pm 0.11	0.78 \pm 0.02	0.00 \pm 0.00	0.00 \pm 0.00	0.00 \pm 0.00
	PRUNE	53.16 \pm 0.17	53.17 \pm 0.14	46.83 \pm 0.15	531.26 \pm 0.22	0.16 \pm 0.05	0.00 \pm 0.00	0.00 \pm 0.00	0.00 \pm 0.00
	RECT	51.92 \pm 0.16	52.03 \pm 0.29	48.03 \pm 0.13	512.85 \pm 1.16	0.37 \pm 0.03	0.00 \pm 0.00	0.01 \pm 0.00	0.00 \pm 0.00
	AlphaEdit	84.59 \pm 0.10	58.41 \pm 0.23	68.96 \pm 0.38	626.15\pm0.60	33.45\pm0.38	97.25\pm0.21	86.17 \pm 0.29	40.16 \pm 0.10
	NAS	90.44\pm0.29	55.05 \pm 0.27	73.21\pm0.22	624.10 \pm 0.28	30.63 \pm 0.37	96.84 \pm 0.23	88.10\pm0.30	42.52\pm0.34
	Pre-edited	15.12 \pm 0.11	17.55 \pm 0.35	83.71 \pm 0.21	622.18 \pm 0.23	29.68 \pm 0.16	27.23 \pm 0.16	26.43 \pm 0.31	27.23 \pm 0.26
GPT-J	FT	57.33 \pm 0.25	<u>54.90\pm0.22</u>	44.75 \pm 0.23	576.65 \pm 0.10	3.09 \pm 0.07	11.85 \pm 0.27	10.26 \pm 0.17	0.51 \pm 0.01
	UltraEdit	56.29 \pm 0.19	49.42 \pm 0.14	51.21 \pm 0.26	498.91 \pm 0.58	14.98 \pm 0.18	65.76 \pm 0.35	62.81 \pm 0.36	28.19\pm0.29
	RLEdit	<u>78.10\pm0.35</u>	54.86 \pm 0.18	48.78 \pm 0.34	<u>579.45\pm0.33</u>	<u>16.76\pm0.36</u>	70.51 \pm 0.26	66.69 \pm 0.34	24.00 \pm 0.29
	MEMIT	49.47 \pm 0.13	49.54 \pm 0.27	50.54 \pm 0.37	509.95 \pm 0.43	4.71 \pm 0.14	2.01 \pm 0.06	0.14 \pm 0.00	0.14 \pm 0.01
	PRUNE	48.86 \pm 0.22	49.01 \pm 0.38	50.94 \pm 0.16	448.54 \pm 1.00	4.74 \pm 0.03	1.06 \pm 0.02	0.03 \pm 0.02	0.03 \pm 0.01
	RECT	48.79 \pm 0.25	48.74 \pm 0.30	51.26 \pm 0.35	240.35 \pm 0.16	4.75 \pm 0.11	0.00 \pm 0.00	0.00 \pm 0.00	0.00 \pm 0.00
	AlphaEdit	62.65 \pm 0.37	54.57 \pm 0.21	<u>54.73\pm0.20</u>	508.65 \pm 0.34	2.90 \pm 0.12	<u>86.13\pm0.23</u>	<u>79.43\pm0.23</u>	21.84 \pm 0.10
	NAS	98.73\pm0.12	90.68\pm0.19	60.75\pm0.22	584.59\pm1.19	40.37\pm0.29	92.08\pm0.33	85.04\pm0.10	22.24 \pm 0.19

4. Experiments

In this section, we evaluate NAS and answer the following research questions (RQs):

- **RQ1.** Across multiple backbone models and datasets under long-horizon *atomic sequential editing*, does NAS achieve superior editing performance and stronger stability compared to existing methods?
- **RQ2.** During long-horizon sequential editing, does NAS better preserve the model’s general capability than existing methods, thereby mitigating degradation on general-purpose tasks?
- **RQ3.** As a plug-and-play component that requires only *a single line of code* to integrate, can NAS suppress norm explosion when attached to different Locate-and-Edit (L&E) baselines, while simultaneously improving editing performance and overall model behavior?

4.1. Experimental Setup

This section briefly describes the datasets, evaluation metrics, backbone models, and baseline methods used in our experiments. Additional details and extended settings are deferred to the appendix A.

Backbone Models. Our main experiments use Llama3-8B(Grattafiori et al., 2024), Qwen2.5-7B(Qwen et al., 2025), and GPT-J(Wang & Komatsuzaki, 2021). As additional backbones, we also conduct supplementary evaluations on GPT2-XL(Radford et al., 2019) (Appendix C.3).

Datasets and Metrics. We adopt two widely used knowledge editing benchmarks, CounterFact (Meng et al., 2023a) and ZsRE (Levy et al., 2017), and follow standard protocols to report *Efficacy*, *Generalization*, *Specificity*, *Fluency*, *Consistency*, and *Score*. To characterize long-horizon failure under sequential editing, we additionally report the *collapse*

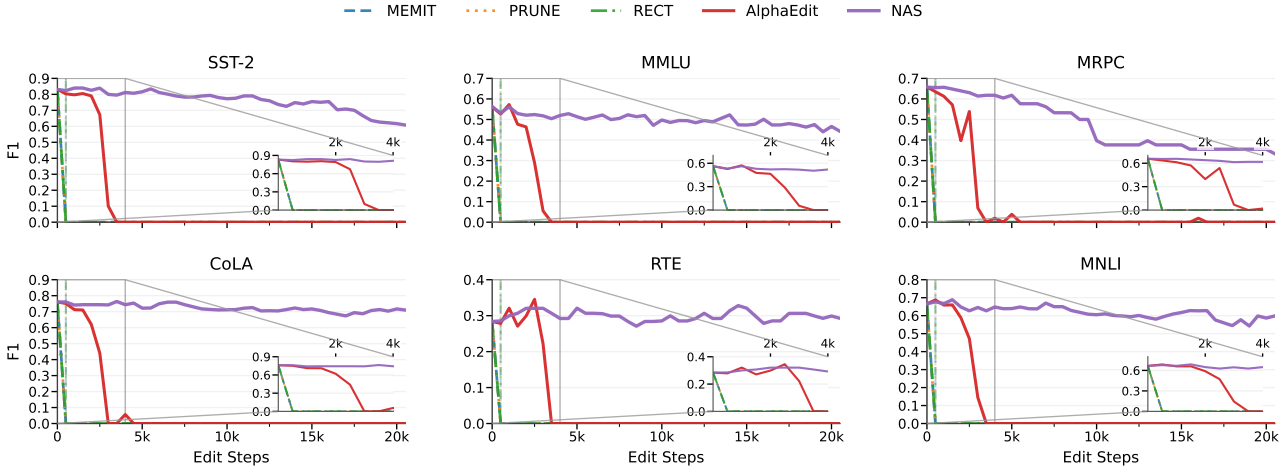


Figure 5. RQ2: GLUE performance (F1) during sequential editing. NAS preserves base-task performance substantially longer than baselines. Insets zoom into the early-edit region (0–4k); inset x-ticks are shown at 2k and 4k for readability.

point (CP@60) (see Appendix A.2.2). We further include WikiBigEdit (Thede et al., 2025), a large-scale benchmark of real-world Wikidata edits, to evaluate longer-horizon sequential editing and to support ablations with additional L&E methods in Appendix C.5.

Baselines. We evaluate a diverse set of baselines spanning both *non-L&E* and *L&E* paradigms. For non-le-in-weight editors, we include FT (Zhu et al., 2020), as well as the recent lifelong editors UltraEdit (Gu et al., 2025) and Rredit (Li et al., 2025). For L&E methods, we include MEMIT (Meng et al., 2023b), PRUNE (Ma et al., 2024), RECT (Gu et al., 2024), and AlphaEdit (Fang et al., 2024). In Appendix C.4, we report results for recent competitive L&E methods ENCORE (Gupta et al., 2025) and LyapLock (Wang et al., 2025b), as official hyperparameters for our main backbones are unavailable. We also report representative *backbone-frozen* editors in Appendix C.4, including GRACE (Hartvigsen et al., 2023), MELO (Yu et al., 2023), WISE (Wang et al., 2024a), and MEMOIR (Wang et al., 2025a).

General language benchmarks. To assess how different editing methods affect the base capabilities of the models, we measure performance on standard language understanding benchmarks during large number of sequential edits. We include GLUE-style tasks (Wang et al., 2019) such as SST (Socher et al., 2013), MRPC (Dolan & Brockett, 2005), RTE (Bentivogli et al., 2009), CoLA (Warstadt et al., 2019), and MNLI (Williams et al., 2018), and MMLU (Hendrycks et al., 2021). (see Appendix A.5 for details).

4.2. Long-horizon Sequential Editing(RQ1)

We evaluate editors under *atomic sequential editing* on the *full* CounterFact (20,877 edits) and ZsRE (19,086 edits)

streams: each request edits exactly one fact and immediately commits a weight update before proceeding to the next. Main results are summarized in Table 1; results on GPT-2XL are provided in Appendix C.3.

Observation 1: NAS yields the strongest long-horizon sequential edit performance. Aggregating results over *both* CounterFact and ZsRE and all three backbones, and comparing each metric to the *strongest baseline under the same evaluation block*, NAS improves edit performance by **+11.5pp** (Eff.) and **+9.9pp** (Gen.) on average, with specificity essentially unchanged (within 0.3pp on average). These gains are consistent with our hidden-representation drift diagnosis (Fig. 4): NAS suppresses the target-layer OOD shift induced by vanilla L&E, and improves long-horizon Eff./Gen. without a stability–strength trade-off despite constraining the update magnitude. NAS also surpasses recent lifelong-focused editors such as ULTRAEDIT and RLEDIT on most metrics, often by a wide margin. The advantage is most pronounced on GPT-J, where NAS boosts CounterFact efficacy from **78.1** to **98.7** (**+20.6pp**) and generalization from **54.9** to **90.7** (**+35.8pp**) over the strongest baseline, while also improving specificity (**54.7** → **60.8**, **+6.0pp**).

Observation 2: NAS maintains fluent generations and improves consistency. Beyond edit performance, NAS remains competitive on *Fluency* while delivering substantially higher *Consistency* under long-horizon sequential editing. Aggregated across the three backbones, NAS improves fluency by **+8.9** and consistency by **+13.5** on average compared to the best baseline within the same evaluation block. The gains are most pronounced on Llama3-8B, where NAS raises fluency from **596.2** to **619.7** (**+23.5**) and boosts consistency from **12.2** to **31.9** (**+19.7**) over the strongest baseline.

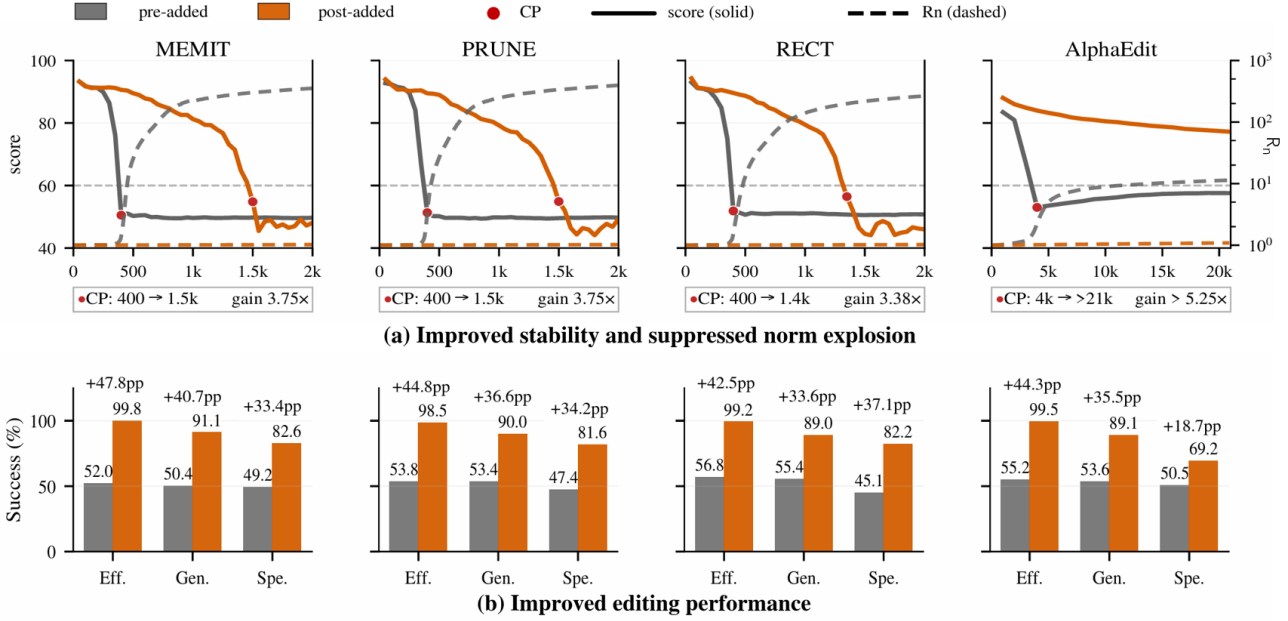


Figure 6. RQ3: NAS improves stability and editing performance under long-horizon sequential editing. (a) Dual-axis trajectories: solid lines show post-edit score, dashed lines show R_n ; the red dot marks the collapse point (CP). (b) Editing quality at baselines’ CP, reported as Eff./Gen./Spe. Comparing pre-added (gray) vs. post-added (orange).

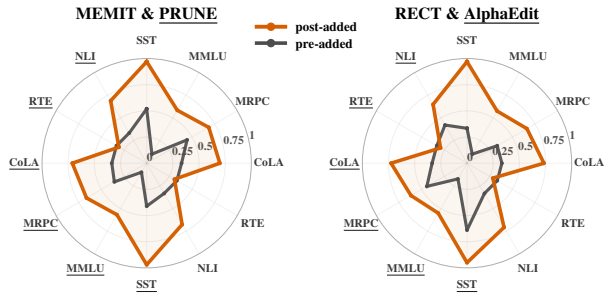


Figure 7. RQ3: General capabilities comparison. Radar plots compare pre-added (gray) and post-added (orange) performance on general capabilities (GLUE-style evaluation) for two method pairs: MEMIT & PRUNE (left) and RECT & AlphaEdit (right). For each radar, the first six axes correspond to the first method in the title, and the underlined six axes correspond to the second method.

4.3. General Capability Retention (RQ2)

To test whether long-horizon sequential editing compromises a model’s *general capability*, we track F1 on *GLUE-style tasks* as edits accumulate. We perform sequential L&E updates over the *entire* CounterFact stream (20,877 edits) for five representative editors (MEMIT, PRUNE, RECT, AlphaEdit, and NAS), and plot the capability trajectories throughout the editing process (Fig. 5; insets zoom into 0–4k edits). We observe consistent trends on additional backbones (Qwen2.5 and GPT-J), with full results in the appendix C.1.

Observation 1: NAS avoids catastrophic capability

degradation. Across the full 20,877-edit stream, NAS maintains *non-trivial* GLUE-style performance without exhibiting catastrophic collapse. Most tasks remain stable over the entire horizon; MRPC shows a more noticeable decline, yet does not degenerate into a near-zero regime.

Observation 2: NAS extends the capability-preserving horizon by $\geq 5\times$. The prior L&E baselines degrade rapidly: their GLUE-style performance drops to near-zero within the first few thousand edits (typically $\leq 4k$). In contrast, NAS extends the capability-preserving horizon from roughly $\sim 4k$ edits to at least 20,877 edits, corresponding to an improvement of *at least* $5\times$.

4.4. Plug-in Gains in Stability and Performance (RQ3)

We evaluate NAS as a plug-in for L&E editors by attaching NAS to four representative L&E baselines with only a *one-line* integration. (MEMIT, PRUNE, RECT, and AlphaEdit) and run long-horizon sequential editing on CounterFact. Main results are reported on Llama3-8B, and we replicate the same study on GPT-J in Appendix C.2. Unless otherwise stated, we report editing quality and general-capability results at a shared reference point—the collapse point (CP) of each corresponding base editor.

Observation 1: NAS suppresses norm explosion and delays collapse across base editors. Figure 6(a) shows dual-axis trajectories during sequential editing, where solid lines track the post-edit score and dashed lines track the norm statistic R_n . Across all four editors, the base variants

exhibit rapid growth in R_n followed by a sharp collapse in score. After integrating NAS, the explosive growth is suppressed and the collapse point is substantially pushed back: $3.75 \times$ for MEMIT and PRUNE (CP: 400 \rightarrow 1.5k), $3.38 \times$ for RECT (400 \rightarrow 1.4k), and $> 5.25 \times$ for AlphaEdit (4k \rightarrow > 21 k). This indicates that NAS acts as a robust stabilization plug-in across heterogeneous L&E update rules.

Observation 2: NAS improves editing quality for each base editor. NAS-augmented editors achieve substantially higher post-edit success on Eff./Gen./Spe. at the reference point, as shown in Fig. 6(b). Averaged across editors and metrics, NAS improves success by **+37.4 percentage points** ($51.9\% \rightarrow 89.3\%$), corresponding to a **+72.2% relative increase**. The gains are broad across efficacy, generalization, and specificity, suggesting that stabilization translates into systematically improved editing behavior rather than isolated wins.

Observation 3: NAS preserves general capability when plugged into base editors. Figure 7 further compares GLUE-style general capability at the same reference point. For both method pairs (MEMIT & PRUNE; RECT & AlphaEdit), the NAS-augmented variants dominate the base editors on most axes; the only near-exception is RTE, where the gap is comparatively small. Overall, NAS improves long-horizon editability by mitigating instability, without sacrificing general capabilities.

5. Related Work

Model editing methods are commonly grouped by whether they *overwrite pretrained weights* (in-weight) or *keep the backbone fixed* and implement edits via auxiliary modules or external memory (Wang et al., 2024b).

In-weight editors (non-L&E). A first line directly optimizes or predicts parameter updates without an explicit locate-then-edit procedure. FT applies standard fine-tuning and can incur broad side effects; MEND meta-learns an editor to transform gradients into more targeted updates (Zhu et al., 2020; Mitchell et al., 2021). Recent lifelong variants include UltraEdit, which computes training-free updates for high-throughput streams; and RLEdit, which trains a hyper-network via reinforcement learning to remain effective as the backbone drifts under sequential edits (Gu et al., 2025; Li et al., 2025).

In-weight editors (Locate-and-Edit). A dominant sub-family follows *Locate-and-Edit* (L&E), applying localized (often low-rank) updates at causal MLP/FFN sites. ROME performs rank-one rewriting (Meng et al., 2023a); MEMIT scales to structured multi-layer updates for mass editing (Meng et al., 2023b); and AlphaEdit constrains update directions/subspaces to reduce interference (Fang

et al., 2024). For long sequential streams, PRUNE and RECT impose stability-oriented constraints (e.g., conditioning/perturbation control or relative-change restriction) to curb degradation (Ma et al., 2024; Gu et al., 2024). ENCORE improves long-horizon L&E with Most-Probable Early Stopping and Frobenius-norm regularization on MEMIT-style updates (Gupta et al., 2025). LyapLock wraps sequential L&E in a Lyapunov-optimization framework to enforce long-run knowledge-preservation constraints (Wang et al., 2025b).

Backbone-frozen editors. Backbone-frozen methods avoid overwriting pretrained weights by storing edits in add-on modules or memory queried at inference. GRACE writes edits into discrete key–value adaptors (Hartvigsen et al., 2023); MELO uses dynamically activated low-rank adapters (Yu et al., 2023); and WISE adopts a dual-memory design with routing to reduce conflicts in lifelong settings (Wang et al., 2024a). MEMOIR store edits in a residual memory with sparse masked updates and selective retrieval to reduce interference (Wang et al., 2025a).

6. Conclusion

In this work, we present the first systematic mechanistic account of *norm explosion* in long-horizon sequential Locate-and-Edit (L&E) editing. By characterizing the recurrence structure induced by mainstream L&E updates, our analysis explains—and enables prediction of—the exponential norm escalation that precipitates long-horizon collapse. Guided by this diagnosis, we introduce NORM-ANCHOR SCALING (NAS), a minimal, plug-and-play modification that anchors the value-vector norm while preserving the update direction, keeping the model within a stable operating regime. Across diverse backbones and benchmarks, supported by competitive baselines and extensive ablations, NAS delivers substantial improvements in long-horizon stability—*dramatically extending the editing lifespan of standard L&E editors*—at negligible overhead while maintaining standard editing quality.

7. Limitation & Future Work

NAS uses a fixed pre-edit anchor to enforce a deliberately minimal form of norm control, demonstrating that constraining value-vector norm growth alone can unlock large gains in long-horizon stability. While this choice improves plug-and-play applicability, a fixed anchor may not be optimal under non-stationary edit streams or for heterogeneous edit difficulty. A natural extension is to develop adaptive or conditional anchoring schemes that adjust the target norm based on the editing context (e.g., edit difficulty, locality, or detected shift), potentially improving robustness without sacrificing simplicity.

Impact Statement

This paper proposes a method to stabilize sequential model editing, enabling Large Language Models (LLMs) to be updated continuously over long horizons without requiring computationally expensive retraining.

Beyond technical efficiency, this work promotes **Environmental Sustainability** as it bypasses the energy-heavy requirement for full-scale retraining to support more sustainable AI infrastructure. Furthermore, it enhances **Systemic Reliability**. In an era where information changes daily, the ability to instantly patch factual errors or safety loopholes is vital for public trust in AI.

However, the power to rewrite model knowledge carries inherent **Risks**. Malicious actors might exploit such efficiency to automate the spread of propaganda or erase sensitive historical facts. Moreover, the long-term cumulative effects of sequential edits on a model’s latent reasoning remain an open question. We emphasize that model editing should be part of a rigorous, supervised pipeline involving continuous integrity checks and transparent access logs.

Conclusion: Researchers and practitioners should implement rigorous access controls and integrity verification mechanisms when deploying model editing interfaces to mitigate the risks of unauthorized tampering.

References

Bentivogli, L., Magnini, B., Dagan, I., Dang, H. T., and Giampiccolo, D. The fifth PASCAL recognizing textual entailment challenge. In *Proceedings of the Second Text Analysis Conference, TAC 2009, Gaithersburg, Maryland, USA, November 16-17, 2009*. NIST, 2009. URL https://tac.nist.gov/publications/2009/additional.papers/RTE5_overview.proceedings.pdf.

De Cao, N., Aziz, W., and Titov, I. Editing factual knowledge in language models. In *Proceedings of the 2021 Conference on Empirical Methods in Natural Language Processing*, pp. 6491–6506, Online and Punta Cana, Dominican Republic, November 2021. Association for Computational Linguistics. doi: 10.18653/v1/2021.emnlp-main.522. URL <https://aclanthology.org/2021.emnlp-main.522/>.

Dhingra, B., Cole, J. R., Eisenschlos, J. M., Gillick, D., Eisenstein, J., and Cohen, W. W. Time-aware language models as temporal knowledge bases. *Transactions of the Association for Computational Linguistics*, 10:257–273, 2022. doi: 10.1162/tacl_a_00459. URL <https://aclanthology.org/2022.tacl-1.15/>.

Dolan, W. B. and Brockett, C. Automatically construct-
ing a corpus of sentential paraphrases. In *Proceedings of the Third International Workshop on Paraphrasing (IWP2005)*, 2005. URL <https://aclanthology.org/I05-5002/>.

Fang, J., Jiang, H., Wang, K., Ma, Y., Jie, S., Wang, X., He, X., and Chua, T.-S. Alphaedit: Null-space constrained knowledge editing for language models. *arXiv preprint arXiv:2410.02355*, 2024.

Geva, M., Schuster, R., Berant, J., and Levy, O. Transformer feed-forward layers are key-value memories, 2021. URL <https://arxiv.org/abs/2012.14913>.

Grattafiori, A., Dubey, A., Jauhri, A., Pandey, A., Kadian, A., Al-Dahle, A., Letman, A., Mathur, A., Schelten, A., Vaughan, A., Yang, A., Fan, A., Goyal, A., Hartshorn, A., Yang, A., Mitra, A., Srivankumar, A., Korenev, A., Hinsvark, A., Rao, A., Zhang, A., Rodriguez, A., Gregerson, A., Spataru, A., Roziere, B., Biron, B., Tang, B., Chern, B., Caucheteux, C., Nayak, C., Bi, C., Marra, C., McConnell, C., Keller, C., Touret, C., Wu, C., Wong, C., Ferrer, C. C., Nikolaidis, C., Allonsius, D., Song, D., Pintz, D., Livshits, D., Wyatt, D., Esiobu, D., Choudhary, D., Mahajan, D., Garcia-Olano, D., Perino, D., Hupkes, D., Lakomkin, E., AlBadawy, E., Lobanova, E., Dinan, E., Smith, E. M., Radenovic, F., Guzmán, F., Zhang, F., Synnaeve, G., Lee, G., Anderson, G. L., Thattai, G., Nail, G., Mialon, G., Pang, G., Cucurell, G., Nguyen, H., Kovera, H., Xu, H., Touvron, H., Zarov, I., Ibarra, I. A., Kloumann, I., Misra, I., Evtimov, I., Zhang, J., Copet, J., Lee, J., Geffert, J., Vranes, J., Park, J., Mahadeokar, J., Shah, J., van der Linde, J., Billock, J., Hong, J., Lee, J., Fu, J., Chi, J., Huang, J., Liu, J., Wang, J., Yu, J., Bitton, J., Spisak, J., Park, J., Rocca, J., Johnstun, J., Saxe, J., Jia, J., Alwala, K. V., Prasad, K., Upasani, K., Plawiak, K., Li, K., Heafield, K., Stone, K., El-Arini, K., Iyer, K., Malik, K., Chiu, K., Bhalla, K., Lakhotia, K., Rantala-Yeary, L., van der Maaten, L., Chen, L., Tan, L., Jenkins, L., Martin, L., Madaan, L., Malo, L., Blecher, L., Landzaat, L., de Oliveira, L., Muzzi, M., Pasupuleti, M., Singh, M., Paluri, M., Kardas, M., Tsimpoukelli, M., Oldham, M., Rita, M., Pavlova, M., Kambadur, M., Lewis, M., Si, M., Singh, M. K., Hassan, M., Goyal, N., Torabi, N., Bashlykov, N., Bogoychev, N., Chatterji, N., Zhang, N., Duchenne, O., Çelebi, O., Alrassy, P., Zhang, P., Li, P., Vasic, P., Weng, P., Bhargava, P., Dubal, P., Krishnan, P., Koura, P. S., Xu, P., He, Q., Dong, Q., Srinivasan, R., Ganapathy, R., Calderer, R., Cabral, R. S., Stojnic, R., Raileanu, R., Maheswari, R., Girdhar, R., Patel, R., Sauvestre, R., Polidoro, R., Sumbaly, R., Taylor, R., Silva, R., Hou, R., Wang, R., Hosseini, S., Chennabasappa, S., Singh, S., Bell, S., Kim, S. S., Edunov, S., Nie, S., Narang, S., Raparthy, S., Shen, S., Wan, S., Bhosale, S., Zhang, S., Vandenhende, S., Batra, S., Whitman, S., Sootla, S.,

Collot, S., Gururangan, S., Borodinsky, S., Herman, T., Fowler, T., Sheasha, T., Georgiou, T., Scialom, T., Speckbacher, T., Mihaylov, T., Xiao, T., Karn, U., Goswami, V., Gupta, V., Ramanathan, V., Kerkez, V., Gonget, V., Do, V., Vogeti, V., Albiero, V., Petrovic, V., Chu, W., Xiong, W., Fu, W., Meers, W., Martinet, X., Wang, X., Wang, X., Tan, X. E., Xia, X., Xie, X., Jia, X., Wang, X., Goldschlag, Y., Gaur, Y., Babaei, Y., Wen, Y., Song, Y., Zhang, Y., Li, Y., Mao, Y., Couder, Z. D., Yan, Z., Chen, Z., Papakipos, Z., Singh, A., Srivastava, A., Jain, A., Kelsey, A., Shajnfeld, A., Gangidi, A., Victoria, A., Goldstand, A., Menon, A., Sharma, A., Boesenberg, A., Baevski, A., Feinstein, A., Kallet, A., Sangani, A., Teo, A., Yunus, A., Lupu, A., Alvarado, A., Caples, A., Gu, A., Ho, A., Poulton, A., Ryan, A., Ramchandani, A., Dong, A., Franco, A., Goyal, A., Saraf, A., Chowdhury, A., Gabriel, A., Bharambe, A., Eisenman, A., Yazdan, A., James, B., Maurer, B., Leonhardi, B., Huang, B., Loyd, B., Paola, B. D., Paranjape, B., Liu, B., Wu, B., Ni, B., Hancock, B., Wasti, B., Spence, B., Stojkovic, B., Gamido, B., Montalvo, B., Parker, C., Burton, C., Mejia, C., Liu, C., Wang, C., Kim, C., Zhou, C., Hu, C., Chu, C.-H., Cai, C., Tindal, C., Feichtenhofer, C., Gao, C., Civin, D., Beaty, D., Kreymer, D., Li, D., Adkins, D., Xu, D., Testuggine, D., David, D., Parikh, D., Liskovich, D., Foss, D., Wang, D., Le, D., Holland, D., Dowling, E., Jamil, E., Montgomery, E., Presani, E., Hahn, E., Wood, E., Le, E.-T., Brinkman, E., Arcaute, E., Dunbar, E., Smothers, E., Sun, F., Kreuk, F., Tian, F., Kokkinos, F., Ozgenel, F., Caggioni, F., Kanayet, F., Seide, F., Florez, G. M., Schwarz, G., Badeer, G., Swee, G., Halpern, G., Herman, G., Sizov, G., Guangyi, Zhang, Lakshminarayanan, G., Inan, H., Shojanazeri, H., Zou, H., Wang, H., Zha, H., Habeeb, H., Rudolph, H., Suk, H., Aspegren, H., Goldman, H., Zhan, H., Damlaj, I., Molybog, I., Tufanov, I., Leontiadis, I., Veliche, I.-E., Gat, I., Weissman, J., Geboski, J., Kohli, J., Lam, J., Asher, J., Gaya, J.-B., Marcus, J., Tang, J., Chan, J., Zhen, J., Reizenstein, J., Teboul, J., Zhong, J., Jin, J., Yang, J., Cummings, J., Carvill, J., Shepard, J., McPhie, J., Torres, J., Ginsburg, J., Wang, J., Wu, K., U, K. H., Saxena, K., Khandelwal, K., Zand, K., Matosich, K., Veeraraghavan, K., Michelena, K., Li, K., Jagadeesh, K., Huang, K., Chawla, K., Huang, K., Chen, L., Garg, L., A, L., Silva, L., Bell, L., Zhang, L., Guo, L., Yu, L., Moshkovich, L., Wehrstedt, L., Khabsa, M., Avalani, M., Bhatt, M., Mankus, M., Hasson, M., Lennie, M., Reso, M., Groshev, M., Naumov, M., Lathi, M., Keneally, M., Liu, M., Seltzer, M. L., Valko, M., Restrepo, M., Patel, M., Vyatskov, M., Samvelyan, M., Clark, M., Macey, M., Wang, M., Hermoso, M. J., Metanat, M., Rastegari, M., Bansal, M., Santhanam, N., Parks, N., White, N., Bawa, N., Singhal, N., Egebo, N., Usunier, N., Mehta, N., Laptev, N. P., Dong, N., Cheng, N., Chernoguz, O., Hart, O., Salpekar, O., Kalinli, O., Kent, P., Parekh, P., Saab, P., Balaji, P., Rittner, P., Bontrager, P., Roux, P., Dollar, P., Zvyagina, P., Ratanchandani, P., Yuvraj, P., Liang, Q., Alao, R., Rodriguez, R., Ayub, R., Murthy, R., Nayani, R., Mitra, R., Parthasarathy, R., Li, R., Hogan, R., Battey, R., Wang, R., Howes, R., Rinott, R., Mehta, S., Siby, S., Bondu, S. J., Datta, S., Chugh, S., Hunt, S., Dhillon, S., Sidorov, S., Pan, S., Mahajan, S., Verma, S., Yamamoto, S., Ramaswamy, S., Lindsay, S., Lindsay, S., Feng, S., Lin, S., Zha, S. C., Patil, S., Shankar, S., Zhang, S., Zhang, S., Wang, S., Agarwal, S., Sajuyigbe, S., Chintala, S., Max, S., Chen, S., Kehoe, S., Satterfield, S., Govindaprasad, S., Gupta, S., Deng, S., Cho, S., Virk, S., Subramanian, S., Choudhury, S., Goldman, S., Remez, T., Glaser, T., Best, T., Koehler, T., Robinson, T., Li, T., Zhang, T., Matthews, T., Chou, T., Shaked, T., Vontimitta, V., Ajayi, V., Montanez, V., Mohan, V., Kumar, V. S., Mangla, V., Ionescu, V., Poenaru, V., Mihailescu, V. T., Ivanov, V., Li, W., Wang, W., Jiang, W., Bouaziz, W., Constable, W., Tang, X., Wu, X., Wang, X., Wu, X., Gao, X., Kleinman, Y., Chen, Y., Hu, Y., Jia, Y., Qi, Y., Li, Y., Zhang, Y., Zhang, Y., Adi, Y., Nam, Y., Yu, Wang, Zhao, Y., Hao, Y., Qian, Y., Li, Y., He, Y., Rait, Z., DeVito, Z., Rosnbrick, Z., Wen, Z., Yang, Z., Zhao, Z., and Ma, Z. The llama 3 herd of models, 2024. URL <https://arxiv.org/abs/2407.21783>.

Gu, J.-C., Xu, H.-X., Ma, J.-Y., Lu, P., Ling, Z.-H., Chang, K.-W., and Peng, N. Model editing harms general abilities of large language models: Regularization to the rescue, 2024. URL <https://arxiv.org/abs/2401.04700>.

Gu, X., Huang, Z., Gu, J.-C., and Zhang, K. Ultraedit: Training-, subject-, and memory-free lifelong editing in language models, 2025. URL <https://arxiv.org/abs/2505.14679>.

Gupta, A., Baskaran, S., and Anumanchipalli, G. Rebuilding rome : Resolving model collapse during sequential model editing, 2024a. URL <https://arxiv.org/abs/2403.07175>.

Gupta, A., Rao, A., and Anumanchipalli, G. K. Model editing at scale leads to gradual and catastrophic forgetting. In *Annual Meeting of the Association for Computational Linguistics*, 2024b. URL <https://api.semanticscholar.org/CorpusID:266999650>.

Gupta, A., Prateepamornkul, P., Lu, M., Alaa, A., Hartvigsen, T., and Anumanchipalli, G. Lifelong knowledge editing requires better regularization, 2025. URL <https://arxiv.org/abs/2502.01636>.

Hartvigsen, T., Sankaranarayanan, S., Palangi, H., Kim, Y., and Ghassemi, M. Aging with grace: Lifelong model

editing with discrete key-value adaptors, 2023. URL <https://arxiv.org/abs/2211.11031>.

Hendrycks, D., Burns, C., Basart, S., Zou, A., Mazeika, M., Song, D., and Steinhardt, J. Measuring massive multitask language understanding, 2021. URL <https://arxiv.org/abs/2009.03300>.

Henry, A., Dachapally, P. R., Pawar, S., and Chen, Y. Query-key normalization for transformers, 2020. URL <https://arxiv.org/abs/2010.04245>.

Levy, O., Seo, M., Choi, E., and Zettlemoyer, L. Zero-shot relation extraction via reading comprehension. *CoRR*, abs/1706.04115, 2017. URL <http://arxiv.org/abs/1706.04115>.

Li, Z., Jiang, H., Chen, H., Bi, B., Zhou, Z., Sun, F., Fang, J., and Wang, X. Reinforced lifelong editing for language models, 2025. URL <https://arxiv.org/abs/2502.05759>.

Lin, S., Hilton, J., and Evans, O. TruthfulQA: Measuring how models mimic human falsehoods. In *Proceedings of the 60th Annual Meeting of the Association for Computational Linguistics (Volume 1: Long Papers)*, pp. 3214–3252, Dublin, Ireland, May 2022. Association for Computational Linguistics. doi: 10.18653/v1/2022.acl-long.229. URL <https://aclanthology.org/2022.acl-long.229>.

Ma, J.-Y., Wang, H., Xu, H.-X., Ling, Z.-H., and Gu, J.-C. Perturbation-restrained sequential model editing. *arXiv preprint arXiv:2405.16821*, 2024.

Meng, K., Bau, D., Andonian, A., and Belinkov, Y. Locating and editing factual associations in gpt, 2023a. URL <https://arxiv.org/abs/2202.05262>.

Meng, K., Sharma, A. S., Andonian, A., Belinkov, Y., and Bau, D. Mass-editing memory in a transformer, 2023b. URL <https://arxiv.org/abs/2210.07229>.

Mitchell, E., Lin, C., Bosselut, A., Finn, C., and Manning, C. D. Fast model editing at scale. *CoRR*, abs/2110.11309, 2021. URL <https://arxiv.org/abs/2110.11309>.

Petroni, F., Rocktäschel, T., Riedel, S., Lewis, P., Bakhtin, A., Wu, Y., and Miller, A. Language models as knowledge bases? In *Proceedings of the 2019 Conference on Empirical Methods in Natural Language Processing and the 9th International Joint Conference on Natural Language Processing (EMNLP-IJCNLP)*, pp. 2463–2473, Hong Kong, China, November 2019. Association for Computational Linguistics. doi: 10.18653/v1/D19-1250. URL https://aclanthology.org/D19-1250.

Qwen, :, Yang, A., Yang, B., Zhang, B., Hui, B., Zheng, B., Yu, B., Li, C., Liu, D., Huang, F., Wei, H., Lin, H., Yang, J., Tu, J., Zhang, J., Yang, J., Yang, J., Zhou, J., Lin, J., Dang, K., Lu, K., Bao, K., Yang, K., Yu, L., Li, M., Xue, M., Zhang, P., Zhu, Q., Men, R., Lin, R., Li, T., Tang, T., Xia, T., Ren, X., Ren, X., Fan, Y., Su, Y., Zhang, Y., Wan, Y., Liu, Y., Cui, Z., Zhang, Z., and Qiu, Z. Qwen2.5 technical report, 2025. URL <https://arxiv.org/abs/2412.15115>.

Radford, A., Wu, J., Child, R., Luan, D., Amodei, D., and Sutskever, I. Language models are unsupervised multitask learners. 2019. URL <https://api.semanticscholar.org/CorpusID:160025533>.

Roberts, A., Raffel, C., and Shazeer, N. How much knowledge can you pack into the parameters of a language model? In *Proceedings of the 2020 Conference on Empirical Methods in Natural Language Processing (EMNLP)*, pp. 5418–5426, Online, November 2020. Association for Computational Linguistics. doi: 10.18653/v1/2020.emnlp-main.437. URL <https://aclanthology.org/2020.emnlp-main.437>.

Scaman, K. and Virmaux, A. Lipschitz regularity of deep neural networks: analysis and efficient estimation, 2019. URL <https://arxiv.org/abs/1805.10965>.

Socher, R., Perelygin, A., Wu, J., Chuang, J., Manning, C. D., Ng, A., and Potts, C. Recursive deep models for semantic compositionality over a sentiment treebank. In *Proceedings of the 2013 Conference on Empirical Methods in Natural Language Processing*, pp. 1631–1642, Seattle, Washington, USA, October 2013. Association for Computational Linguistics. URL <https://aclanthology.org/D13-1170>.

Takase, S., Kiyono, S., Kobayashi, S., and Suzuki, J. Spike no more: Stabilizing the pre-training of large language models, 2025. URL <https://arxiv.org/abs/2312.16903>.

Thede, L., Roth, K., Bethge, M., Akata, Z., and Hartvigsen, T. WikiBigEdit: Understanding the Limits of Lifelong Knowledge Editing in LLMs. In *Proceedings of the 42nd International Conference on Machine Learning (ICML)*, 2025.

Wang, A., Singh, A., Michael, J., Hill, F., Levy, O., and Bowman, S. R. Glue: A multi-task benchmark and analysis platform for natural language understanding, 2019. URL <https://arxiv.org/abs/1804.07461>.

Wang, B. and Komatsuzaki, A. GPT-J-6B: A 6 Billion Parameter Autoregressive Language Model. <https://github.com/kingoflolz/mesh-transformer-jax>, May 2021.

Wang, K., Qin, Y., Dimitriadis, N., Favero, A., and Frossard, P. Memoir: Lifelong model editing with minimal overwrite and informed retention for llms, 2025a. URL <https://arxiv.org/abs/2506.07899>.

Wang, P., Li, Z., Zhang, N., Xu, Z., Yao, Y., Jiang, Y., Xie, P., Huang, F., and Chen, H. Wise: Rethinking the knowledge memory for lifelong model editing of large language models, 2024a. URL <https://arxiv.org/abs/2405.14768>.

Wang, P., Zhou, B., Tang, X., Han, J., and Hu, S. Lyaplock: Bounded knowledge preservation in sequential large language model editing, 2025b. URL <https://arxiv.org/abs/2505.15702>.

Wang, S., Zhu, Y., Liu, H., Zheng, Z., Chen, C., and Li, J. Knowledge editing for large language models: A survey, 2024b. URL <https://arxiv.org/abs/2310.16218>.

Warstadt, A., Singh, A., and Bowman, S. R. Neural network acceptability judgments. *Transactions of the Association for Computational Linguistics*, 7:625–641, 2019. doi: 10.1162/tacl_a_00290. URL <https://aclanthology.org/Q19-1040/>.

Williams, A., Nangia, N., and Bowman, S. A broad-coverage challenge corpus for sentence understanding through inference. In *Proceedings of the 2018 Conference of the North American Chapter of the Association for Computational Linguistics: Human Language Technologies, Volume 1 (Long Papers)*, pp. 1112–1122, New Orleans, Louisiana, June 2018. Association for Computational Linguistics. doi: 10.18653/v1/N18-1101. URL <https://aclanthology.org/N18-1101/>.

Xiong, R., Yang, Y., He, D., Zheng, K., Zheng, S., Xing, C., Zhang, H., Lan, Y., Wang, L., and Liu, T.-Y. On layer normalization in the transformer architecture, 2020. URL <https://arxiv.org/abs/2002.04745>.

Xu, H.-X., Ma, J.-Y., Ling, Z.-H., Zhang, N., and Gu, J.-C. Constraining sequential model editing with editing anchor compression, 2025. URL <https://arxiv.org/abs/2503.00035>.

Yao, Y., Wang, P., Tian, B., Cheng, S., Li, Z., Deng, S., Chen, H., and Zhang, N. Editing large language models: Problems, methods, and opportunities. In *Proceedings of the 2023 Conference on Empirical Methods in Natural Language Processing*, pp. 10222–10240, Singapore, December 2023. Association for Computational Linguistics. doi: 10.18653/v1/2023.emnlp-main.632. URL <https://aclanthology.org/2023.emnlp-main.632/>.

Yu, L., Chen, Q., Zhou, J., and He, L. Melo: Enhancing model editing with neuron-indexed dynamic lora, 2023. URL <https://arxiv.org/abs/2312.11795>.

Zhang, T., Kang, H., Li, D., Chen, Q., He, C. W. X., and Hong, R. Queueedit: Structural self-correction for sequential model editing in llms, 2025. URL <https://arxiv.org/abs/2506.17864>.

Zhang, X. and Wu, J. Dissecting learning and forgetting in language model finetuning. In *The Twelfth International Conference on Learning Representations*, 2024. URL <https://openreview.net/forum?id=tmsqb6WpLz>.

Zhu, C., Rawat, A. S., Zaheer, M., Bhojanapalli, S., Li, D., Yu, F. X., and Kumar, S. Modifying memories in transformer models. *CoRR*, abs/2012.00363, 2020. URL <https://arxiv.org/abs/2012.00363>.

A. Experimental Setup and Implement Details

In this section, we describe the datasets and evaluation metrics used in our experiments, and detail the base-model capability evaluation, experimental setup, and baseline methods.

A.1. Datasets

- **CounterFact.** CounterFact(Meng et al., 2023a) is a benchmark designed specifically for *factual knowledge editing*. Each example specifies a factual triple in the form of a *subject* and *relation* (e.g., “Paris is the capital of France”) together with a *counterfactual target object* to be written into the model (e.g., replacing France with a new object). The benchmark provides multiple prompt variants to query the edited knowledge (e.g., a direct rewrite prompt and paraphrases), as well as semantically related “neighborhood” prompts used to check locality/specificity. It is therefore commonly used to measure whether an editor succeeds on the intended rewrite while preserving behavior on nearby but non-target facts.
- **ZsRE.** ZsRE(Levy et al., 2017) is a widely used factual probing dataset derived from relation extraction in a *question-answering* format. Each instance corresponds to a (subject, relation) query rendered as a natural-language question (often with paraphrased variants), and the model is expected to generate the correct answer entity. In model editing, ZsRE is typically used to evaluate whether an edit can reliably update the answer to a targeted question while generalizing across question paraphrases, making it a complementary benchmark to CounterFact for assessing efficacy and generalization under diverse query formulations.
- **WikiBigEdit.** WikiBigEdit(Thede et al., 2025) is a large-scale *lifelong* knowledge-editing benchmark constructed from real-world Wikidata snapshot *diffs*, yielding a chronological stream of factual changes with over 500K question–answer pairs. Each example is grounded in a Wikidata (subject, relation, object) triplet and provides an *update* question plus rephrases/persona variants to test generalization; it further includes dedicated *locality* prompts (with expected answers) and optional *multi-hop* questions to probe whether edits preserve unrelated knowledge and reasoning behavior.

A.2. Metrics

We report standard knowledge-editing metrics on ZsRE and COUNTERFACT, and additionally introduce a long-horizon stability indicator based on the CounterFact score. We also report WIKIBIGEDIT metrics following the official benchmark protocol, namely *Edit Success* (ES), *Generalization Success* (GS), and *Locality Success* (LS). For each edit instance i , let f_θ denote the (edited) language model, (s_i, r_i) the edit prompt constructed from the subject–relation pair, and o_i the desired post-edit target output. We use $N((s_i, r_i))$ to denote a set of paraphrased (semantically equivalent) prompts, and $O((s_i, r_i))$ to denote a set of locality prompts used to probe non-target behavior. In sequential-editing experiments, metrics are evaluated at a set of discrete checkpoints (shared across all methods for a fixed base model), which enables us to define the *collapse point* (CP) as the first checkpoint where the CounterFact score falls below a predefined threshold. Our definitions largely follow common practice in prior work (e.g., (Meng et al., 2023a;b; Zhang et al., 2025; Fang et al., 2024)), but we restate them here for completeness.

A.2.1. ZsRE METRICS

Efficacy. On ZsRE, efficacy is measured as the average top-1 accuracy on the edited questions:

$$\mathbb{E}_i \left\{ o_i = \arg \max_o \mathbb{P}_{f_\theta}(o \mid (s_i, r_i)) \right\}. \quad (17)$$

Generalization. Generalization evaluates whether the edit transfers to paraphrased queries. We compute the average top-1 accuracy over the rephrased prompt set $N((s_i, r_i))$:

$$\mathbb{E}_i \left\{ o_i = \arg \max_o \mathbb{P}_{f_\theta}(o \mid N((s_i, r_i))) \right\}. \quad (18)$$

Specificity (Locality). Specificity captures whether the edit avoids changing predictions on locality prompts $O((s_i, r_i))$. We evaluate this by checking whether the model’s top-1 prediction on $O((s_i, r_i))$ matches the (original) pre-edit answer o_i^c :

$$\mathbb{E}_i \left\{ o_i^c = \arg \max_o \mathbb{P}_{f_\theta}(o \mid O((s_i, r_i))) \right\}. \quad (19)$$

A.2.2. COUNTERFACT METRICS

On COUNTERFACT, the evaluation is likelihood-based. let o_c^i be the model’s original (pre-edit) output for the edit prompt, and o_i the desired new object to be written. We then define:

Efficacy (Rewrite Success). We count an edit as successful on the rewrite prompt if the new target is assigned higher probability than the original output:

$$\mathbb{E}_i [\mathbb{P}_{f_\theta}[o_i | (s_i, r_i)] > \mathbb{P}_{f_\theta}[o_c^i | (s_i, r_i)]] . \quad (20)$$

Generalization (Paraphrase Success). We analogously evaluate paraphrase generalization on the rephrased prompt set $N((s_i, r_i))$:

$$\mathbb{E}_i [\mathbb{P}_{f_\theta}[o_i | N((s_i, r_i))] > \mathbb{P}_{f_\theta}[o_c^i | N((s_i, r_i))]] . \quad (21)$$

Specificity (Neighborhood/Locality Success). Specificity is computed on neighborhood prompts $O((s_i, r_i))$ (distinct but semantically related subjects) by requiring the edited model to favor the correct/original completion over the edited target:

$$\mathbb{E}_i [\mathbb{P}_{f_\theta}[o_i | O((s_i, r_i))] > \mathbb{P}_{f_\theta}[o_c^i | O((s_i, r_i))]] . \quad (22)$$

Score (Harmonic Mean). In addition to reporting *Efficacy*, *Generalization*, and *Specificity* separately, we also summarize CounterFact performance with a single *overall score* defined as their harmonic mean:

$$\text{Score} := H(\text{Eff.}, \text{Gen.}, \text{Spe.}) = \frac{3}{\frac{1}{\text{Eff.}} + \frac{1}{\text{Gen.}} + \frac{1}{\text{Spe.}}} . \quad (23)$$

Here, Eff., Gen., and Spe. are the dataset-level success rates defined above (Eqs. 20–22).

Collapse Point (CP@60). let $\mathcal{T}_m = \{t_1, t_2, \dots\}$ be the evaluation checkpoints for base model m , and let $\text{Score}(t)$ denote the CounterFact score at checkpoint t . We define the collapse point as the earliest checkpoint where the score falls below a threshold:

$$\text{CP@60} := \min \{t \in \mathcal{T}_m : \text{Score}(t) \leq 60\} . \quad (24)$$

Due to discrete evaluation, the true collapse (if any) occurs within the interval $(t^-, \text{CP@60}]$, where t^- is the immediate predecessor of CP@60 in \mathcal{T}_m .

Fluency (Generation Entropy). To detect degenerate generations with excessive repetition, we compute an n -gram entropy score:

$$-\frac{2}{3} \sum_k g_2(k) \log_2 g_2(k) + \frac{4}{3} \sum_k g_3(k) \log_2 g_3(k), \quad (25)$$

where $g_n(\cdot)$ denotes the empirical frequency distribution of n -grams in the model output.

Consistency (Reference Score). Consistency evaluates whether the model’s generated description remains aligned with a reference text. Given a subject s , we compute the cosine similarity between the TF-IDF vector of the model-generated text and that of a reference Wikipedia passage about the corresponding object.

A.2.3. WIKIBIGEDIT METRICS

On WIKIBIGEDIT, the evaluation is accuracy-based on question–answer prompts. For each edit instance i , let (s_i, r_i) denote the update query, and o_i the desired post-edit target output. We use $N((s_i, r_i))$ to denote a set of generalization queries (e.g., rephrases/persona variants), and $O((s_i, r_i))$ to denote a set of locality probes paired with edit i , whose answers should remain unchanged (denoted by o_i^c).

ES (Edit Success). We measure edit success as the average top-1 accuracy on the update queries:

$$\mathbb{E}_i \left\{ o_i = \arg \max_o \mathbb{P}_{f_\theta}(o | (s_i, r_i)) \right\} . \quad (26)$$

GS (Generalization Success). Generalization evaluates whether the edit transfers to the associated generalization set $N((s_i, r_i))$:

$$\mathbb{E}_i \left\{ o_i = \arg \max_o \mathbb{P}_{f_\theta}(o \mid N((s_i, r_i))) \right\}. \quad (27)$$

LS (Locality Success). Locality evaluates whether predictions on paired locality probes $O((s_i, r_i))$ match their original (pre-edit) answers o_i^c :

$$\mathbb{E}_i \left\{ o_i^c = \arg \max_o \mathbb{P}_{f_\theta}(o \mid O((s_i, r_i))) \right\}. \quad (28)$$

A.3. Implementation details

Table 2. Ablation on hyperparameter N (5 restarts). We report runtime (seconds; mean \pm sample std) and the raw-mean estimate of $\|v^{\text{new}}\|$ (mean \pm std).

Model	N	Time (s)	Raw $\ v^{\text{new}}\ $
Llama3-8B	100	47.15 ± 5.68	5.298 ± 0.040
	300	143.33 ± 1.95	5.309 ± 0.019
	500	239.13 ± 4.05	5.320 ± 0.020
	1000	469.34 ± 6.81	5.325 ± 0.015
	2000	936.79 ± 8.51	5.322 ± 0.007
GPT-J-6B	100	13.07 ± 1.57	63.248 ± 1.102
	300	41.43 ± 1.37	62.872 ± 0.634
	500	67.84 ± 2.54	62.946 ± 0.561
	1000	135.06 ± 1.78	63.075 ± 0.412
	2000	268.83 ± 2.99	63.038 ± 0.179

Estimating the anchor norm. NAS requires a single scalar anchor level $a := \mathbb{E}\|v^{\text{new}}\|^2$ measured on a clean (unedited) model. In all experiments, we estimate this expectation by performing pilot edits on $N = 1000$ randomly sampled facts and computing the empirical mean of the resulting $\|v^{\text{new}}\|^2$ values. We use the same editing site and the same base editor configuration as in the main sequential-editing runs.

Integration with base editors. NAS is implemented as a lightweight post-processing step on the target value vector produced by the base editor. When inserting NAS into an editor, we only introduce two NAS-specific hyperparameters: (i) the pilot sample size N (fixed to 1000 throughout this paper), and (ii) a boolean flag `use_nas` indicating whether to enable the rescaling rule. All other hyperparameters and logic—including the computation of \tilde{v}_n^{new} , optimization settings, and update rules—are inherited *unchanged* from the attached editor. Unless otherwise stated, when we refer to “NAS” as an independent editing method, it denotes **AlphaEdit** equipped with NAS (i.e., AlphaEdit + NAS).

Sensitivity to N . We ablate the hyperparameter N over $\{100, 300, 500, 1000, 2000\}$ with 5 restarts. Across both Llama3-8B and GPT-J-6B, the raw-mean estimate of $\|v^{\text{new}}\|$ remains highly stable as N increases (e.g., Llama3-8B varies only from 5.298 at $N=100$ to 5.322 at $N=2000$, and GPT-J-6B stays within 62.87–63.25), with variability across restarts generally shrinking for larger N . In contrast, the runtime increases approximately linearly with N (e.g., on Llama3-8B from 47.15s at $N=100$ to 936.79s at $N=2000$), indicating that larger N primarily trades compute for marginally reduced estimator variance rather than changing the central tendency.

Compute resources. All experiments were conducted on a single NVIDIA H100 GPU. For in-weight Locate-and-Edit (L&E) editors (e.g., ROME/MEMIT/PRUNE/RECT/AlphaEdit), running sequential editing on our primary base models typically requires at least 48 GB of GPU memory due to the model size and the per-edit optimization/update procedure. Importantly, enabling NAS does not introduce additional GPU-memory overhead.

A.4. Baselines

All baselines are evaluated using the **official implementations and recommended hyperparameters released by the authors**. The only exception is PRUNE, for which we use the implementation provided in the **AlphaEdit** codebase (Fang et al., 2024).

- **FT (Fine-Tuning).** (Zhu et al., 2020) A straightforward baseline that directly fine-tunes the model on the edited fact via gradient-based optimization. While often effective at rewriting the target behavior, standard fine-tuning can introduce broader parameter changes and thus may cause unintended side effects on unrelated knowledge.
- **MEMIT.** (Meng et al., 2023b) A scalable in-weight editing method designed for efficiently injecting many factual updates. It generalizes single-edit rank-constrained updates to multi-edit settings by composing a structured weight update (often distributed across layers), enabling large batches or long streams of edits with improved efficiency.
- **PRUNE.** (Ma et al., 2024) A regularization-based editor that constrains edit-induced perturbations to preserve model fidelity under sequential updates. It controls the geometry (e.g., update conditioning) of the applied change to suppress overly aggressive directions, thereby mitigating degradation and side effects over long edit horizons.
- **RECT.** (Gu et al., 2024) An editing method that restricts the relative change of weights during an update, typically by sparsifying or truncating the weight delta so that only the most relevant subset of parameters is modified. This strategy retains the base model’s general capabilities while still achieving high edit efficacy on the target knowledge.
- **AlphaEdit.** (Fang et al., 2024) A constrained in-weight editor that shapes the update to reduce interference with pre-existing knowledge. It enforces an approximate invariance constraint (e.g., a null-space projection) so that the update primarily affects the target association while minimizing unintended changes to other facts.
- **UltraEdit.** (Gu et al., 2025) A training- and memory-free editing method that computes the weight update in a single step from a hidden state and its gradient, without any additional fine-tuning. UltraEdit also employs a continual feature normalization strategy to adapt to distribution shifts across sequential edits, enabling ultra-fast and scalable knowledge updates with minimal interference.
- **Rredit.** (Li et al., 2025) A reinforcement learning-based editor that formulates sequential model editing as a decision process for a hypernetwork. By treating editing success as a reward and optimizing the hypernetwork over entire edit sequences, Rredit adapts to dynamic model changes and achieves superior editing efficacy and efficiency in lifelong settings.
- **GRACE.** (Hartvigsen et al., 2023) A lifelong editing approach that stores new knowledge in auxiliary key-value style adapters rather than modifying backbone parameters. Each edit is written into a dedicated latent adapter, and a retrieval mechanism activates the corresponding adapter for relevant inputs, supporting a large number of edits with reduced interference on original knowledge.
- **MELO.** (Yu et al., 2023) A plug-in editor that realizes edits via dynamically activated low-rank adapters (e.g., LoRA-style modules). New facts are stored in separate adapter modules that are selectively invoked for matching inputs, providing modularity and strong isolation of edits without changing the core model weights.
- **WISE.** (Wang et al., 2024a) A dual-memory approach that separates original knowledge retention from edited knowledge storage. It writes updates into an auxiliary “side” memory and uses a routing mechanism to combine or choose between the base model and the edited memory at inference time, aiming to reduce interference and improve stability under continual updates.
- **LyapLock.** (Wang et al., 2025b) A sequential L&E wrapper that formulates editing as a long-term constrained optimization problem and uses Lyapunov optimization (virtual queues) to enforce cumulative knowledge-preservation constraints while remaining compatible with existing editors.
- **ENCORE.** (Gupta et al., 2025) A regularization-oriented L&E extension that combines Most-Probable Early Stopping (MPES) with Frobenius-norm regularization on MEMIT-style closed-form updates to mitigate over-optimization and norm growth in long edit streams.
- **MEMOIR.** (Wang et al., 2025a) A backbone-frozen lifelong editor that writes edits into a residual memory module via sparse, sample-dependent masked updates (TopHash) and selectively retrieves relevant memory at inference to reduce interference.

A.5. General Capability Evaluation

Beyond edit-centric metrics, we also monitor whether long streams of edits erode the base model’s *general-purpose* language understanding and reasoning ability. This type of collateral degradation under (lifelong) sequential editing has been repeatedly observed in recent evaluations of model editing at scale, motivating routine reporting of downstream benchmark performance alongside editing success (Fang et al., 2024; Zhang et al., 2025). Following this common practice, we evaluate the edited model on five representative tasks from GLUE (Wang et al., 2019) and on MMLU (Hendrycks et al., 2021) at a set of checkpoints during the edit stream.

- **SST-2 (SST).** A sentence-level sentiment classification task derived from movie reviews. The model predicts whether a review expresses *positive* or *negative* sentiment, probing basic lexical and compositional understanding as well as robustness to stylistic variation.
- **MRPC.** The Microsoft Research Paraphrase Corpus is a sentence-pair task that asks whether two sentences are paraphrases (i.e., semantically equivalent). It serves as a compact probe of semantic similarity judgments and sensitivity to small meaning changes.
- **RTE.** Recognizing Textual Entailment is a binary natural language inference (NLI) task. Given a premise and a hypothesis, the model predicts whether the hypothesis is entailed by the premise, providing a probe of logical/semantic inference under limited supervision.
- **CoLA.** The Corpus of Linguistic Acceptability asks whether a sentence is grammatically acceptable. While GLUE commonly reports MCC for CoLA, we compute F1 on the acceptability label to keep a unified scale across tasks; this benchmark primarily serves as a probe of syntactic/grammatical sensitivity.
- **MNLI.** Multi-Genre Natural Language Inference is a three-way NLI classification task (entailment/neutral/contradiction) spanning diverse text domains. It is a stronger, broader probe of inference capability than RTE and is commonly used as a barometer of general sentence-pair understanding.
- **MMLU.** Measuring Massive Multitask Language Understanding is a multiple-choice benchmark covering a broad set of academic and professional subjects. Each example presents a question with a fixed set of answer options, testing both factual knowledge and multi-step reasoning in a standardized format.

B. Proofs and Derivations

B.1. Definitions and Basic Identities

Our analysis studies the dynamical evolution of $\|v_n^{\text{old}}\|^2$, $\|v_n^{\text{new}}\|^2$, and $\|W_n\|_F^2$ under sequential edits. We first recall the definition of the Frobenius norm and inner product, together with several identities that will be used repeatedly.

Definition B.1 (Frobenius norm). For any real matrix $A \in \mathbb{R}^{m \times n}$ with entries $(A)_{ij} = a_{ij}$, the Frobenius norm is

$$\|A\|_F^2 := \sum_{i=1}^m \sum_{j=1}^n a_{ij}^2. \quad (29)$$

Equivalently, $\|A\|_F$ is the Euclidean norm of $\text{vec}(A) \in \mathbb{R}^{mn}$. For convenience, we use $\|A\|^2$ to denote $\|A\|_F^2$ when the meaning is clear.

Definition B.2 (Frobenius inner product). For any $A, B \in \mathbb{R}^{m \times n}$ with entries $(A)_{ij} = a_{ij}$ and $(B)_{ij} = b_{ij}$, the Frobenius inner product is

$$\langle A, B \rangle_F := \sum_{i=1}^m \sum_{j=1}^n a_{ij} b_{ij}. \quad (30)$$

This coincides with the Euclidean inner product between $\text{vec}(A)$ and $\text{vec}(B)$, and in particular

$$\|A\|_F^2 = \langle A, A \rangle_F. \quad (31)$$

lemma B.3 (Useful identities). *For any $A, B \in \mathbb{R}^{m \times n}$, $u \in \mathbb{R}^m$, and $v \in \mathbb{R}^n$, the following hold:*

$$\|A + B\|_F^2 = \|A\|_F^2 + \|B\|_F^2 + 2\langle A, B \rangle_F, \quad (32)$$

$$\|uv^\top\|_F^2 = \|u\|^2 \|v\|^2, \quad (33)$$

$$\langle A, uv^\top \rangle_F = u^\top Av. \quad (34)$$

B.2. Proof for lemma 3.1

Recall that under the convention $C = I$, Eq. (10) can be written as Eq. (11):

$$\Delta W_n = \frac{(v_n^{\text{new}} - v_n^{\text{old}}) k_n^* \top}{\|k_n^*\|^2}. \quad (35)$$

Starting from Eq. (8) and applying the Frobenius identity (32) (lemma B.3), we have

$$\begin{aligned} \|W_n\|^2 &= \|W_{n-1} + \Delta W_n\|^2 \\ &= \|W_{n-1}\|^2 + \|\Delta W_n\|^2 + 2\langle W_{n-1}, \Delta W_n \rangle_F. \end{aligned} \quad (36)$$

We now expand the last two terms in Eq. (36). First, by Eq. (33) (lemma B.3) and (11),

$$\begin{aligned} \|\Delta W_n\|^2 &= \left\| \frac{(v_n^{\text{new}} - v_n^{\text{old}}) k_n^* \top}{\|k_n^*\|^2} \right\|^2 \\ &= \frac{\|v_n^{\text{new}} - v_n^{\text{old}}\|^2}{\|k_n^*\|^2}. \end{aligned} \quad (37)$$

Second, by Eq. (34) (lemma B.3) and (11),

$$\begin{aligned} \langle W_{n-1}, \Delta W_n \rangle_F &= \left\langle W_{n-1}, \frac{(v_n^{\text{new}} - v_n^{\text{old}}) k_n^* \top}{\|k_n^*\|^2} \right\rangle_F \\ &= \frac{1}{\|k_n^*\|^2} \left\langle W_{n-1}, (v_n^{\text{new}} - v_n^{\text{old}}) k_n^* \right\rangle_F \\ &= \frac{1}{\|k_n^*\|^2} (v_n^{\text{new}} - v_n^{\text{old}})^\top W_{n-1} k_n^*. \end{aligned} \quad (38)$$

Substituting Eqs. (37) and (38) into Eq. (36) yields

$$\|W_n\|^2 = \|W_{n-1}\|^2 + \frac{\|v_n^{\text{new}} - v_n^{\text{old}}\|^2}{\|k_n^*\|^2} + \frac{2}{\|k_n^*\|^2} (v_n^{\text{new}} - v_n^{\text{old}})^\top W_{n-1} k_n^*. \quad (39)$$

Recall that $v_n^{\text{old}} = W_{n-1} k_n^*$, and define $\Delta_n := v_n^{\text{new}} - v_n^{\text{old}}$. Then Eq. (39) becomes

$$\|W_n\|^2 = \|W_{n-1}\|^2 + \frac{1}{\|k_n^*\|^2} \left(\|\Delta_n\|^2 + 2\langle \Delta_n, v_n^{\text{old}} \rangle \right). \quad (40)$$

Finally, since $v_n^{\text{new}} = v_n^{\text{old}} + \Delta_n$,

$$\|\Delta_n\|^2 + 2\langle \Delta_n, v_n^{\text{old}} \rangle = \|v_n^{\text{new}}\|^2 - \|v_n^{\text{old}}\|^2. \quad (41)$$

Plugging Eq. (41) into Eq. (40) gives exactly Eq. (12), completing the proof.

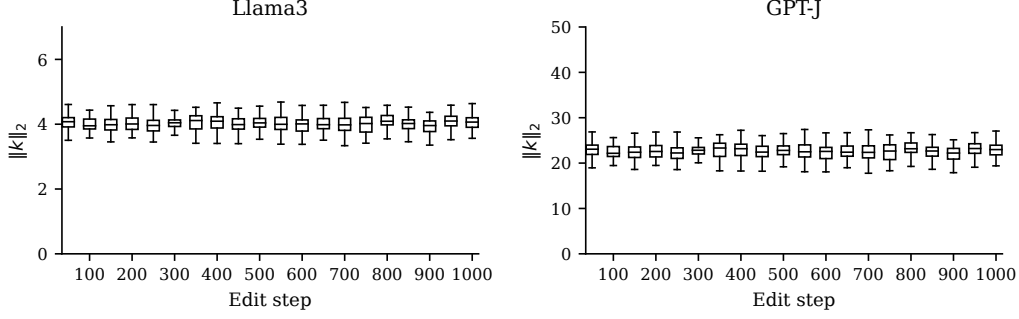


Figure 8. $\|k_n^*\|^2$ stability across edit steps. Boxplots of $\|k_n^*\|$ over edit steps show small fluctuation and tight concentration, supporting the approximation $\|k_n^*\|^2 \approx K$ used in the analysis.

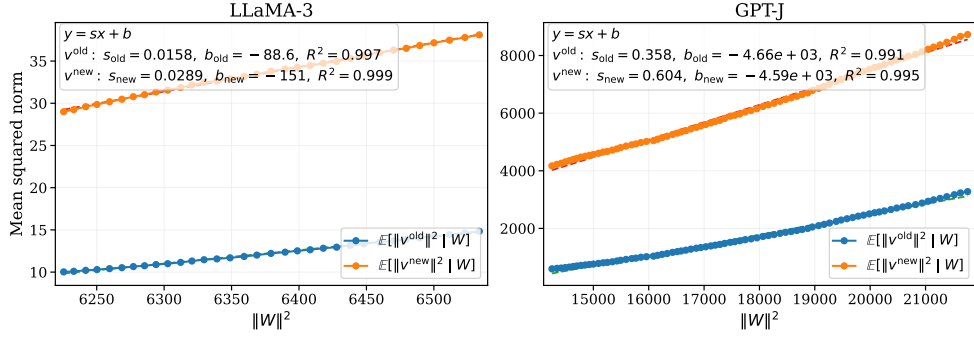


Figure 9. Linear scaling between value-vector norms and the edited weight norm (baseline). For sequential editing, we plot $\mathbb{E}[\|v_n^{\text{new}}\|^2 | W]$ and $\mathbb{E}[\|v_n^{\text{old}}\|^2 | W]$ versus $\|W\|^2$ at multiple checkpoints (averaged over sampled edits/keys). Dashed lines are linear fits; insets report fitted slopes and R^2 . The fitted slope for v_n^{new} is consistently larger than that for v_n^{old} .

B.3. Proof for Prop. 3.2

Starting from lemma 3.1 (Eq. (12)), we take conditional expectation given the current weight W_{n-1} :

$$\mathbb{E}[\|W_n\|^2 | W_{n-1}] = \|W_{n-1}\|^2 + \mathbb{E}\left[\frac{\|v_n^{\text{new}}\|^2 - \|v_n^{\text{old}}\|^2}{\|k_n^*\|^2} \mid W_{n-1}\right]. \quad (42)$$

Empirically, $\|k_n^*\|$ varies little across edit steps (Fig. 8). We therefore treat $\|k_n^*\|^2$ as approximately constant and set

$$K := \text{the empirical mean of } \|k_n^*\|^2 \text{ over the sampled checkpoints and sampled edits/keys.} \quad (43)$$

Substituting $\|k_n^*\|^2 \approx K$ into (42) yields

$$\mathbb{E}[\|W_n\|^2 | W_{n-1}] \approx \|W_{n-1}\|^2 + K \cdot \mathbb{E}[\|v_n^{\text{new}}\|^2 - \|v_n^{\text{old}}\|^2 | W_{n-1}]. \quad (44)$$

Next, Fig. 9 shows an approximately linear scaling between value-vector norms and the edited weight norm over the observation range:

$$\mathbb{E}[\|v_n^{\text{new}}\|^2 | W_{n-1}] \approx s_{\text{new}} \|W_{n-1}\|^2 + b_{\text{new}}, \quad (45)$$

$$\mathbb{E}[\|v_n^{\text{old}}\|^2 | W_{n-1}] \approx s_{\text{old}} \|W_{n-1}\|^2 + b_{\text{old}}, \quad (46)$$

where $s_{\text{new}} > s_{\text{old}} > 0$.

Subtracting Eq. (46) from Eq. (45) gives

$$\mathbb{E}[\|v_n^{\text{new}}\|^2 - \|v_n^{\text{old}}\|^2 | W_{n-1}] \approx (s_{\text{new}} - s_{\text{old}}) \|W_{n-1}\|^2 + (b_{\text{new}} - b_{\text{old}}). \quad (47)$$

For notational convenience, we introduce a unified reparametrization of the empirical linear fits by the two constants (ρ, γ) :

$$\rho(s_{\text{new}}, s_{\text{old}}; K) := 1 + K(s_{\text{new}} - s_{\text{old}}), \quad \gamma(s_{\text{new}}, b_{\text{new}}, s_{\text{old}}, b_{\text{old}}) := \frac{b_{\text{new}} - b_{\text{old}}}{s_{\text{new}} - s_{\text{old}}}. \quad (48)$$

Then Eq. (47) can be rewritten as

$$\mathbb{E}[\|v_n^{\text{new}}\|^2 - \|v_n^{\text{old}}\|^2 \mid W_{n-1}] \approx (s_{\text{new}} - s_{\text{old}})(\|W_{n-1}\|^2 + \gamma), \quad \text{where } \gamma = \gamma(s_{\text{new}}, b_{\text{new}}, s_{\text{old}}, b_{\text{old}}) \quad (49)$$

Substituting Eq. (49) into Eq. (44) yields

$$\mathbb{E}[\|W_n\|^2 \mid W_{n-1}] \approx \|W_{n-1}\|^2 + K(s_{\text{new}} - s_{\text{old}})(\|W_{n-1}\|^2 + \gamma) = \rho \|W_{n-1}\|^2 + (\rho - 1)\gamma, \quad \text{where } \rho = \rho(s_{\text{new}}, s_{\text{old}}; K). \quad (50)$$

Taking expectation on both sides and using the tower property,

$$\mathbb{E}\|W_n\|^2 \approx \rho \mathbb{E}\|W_{n-1}\|^2 + (\rho - 1)\gamma. \quad (51)$$

Since $K > 0$ and $s_{\text{new}} - s_{\text{old}} > 0$, we have $\rho > 1$. Solving Eq. (51) gives

$$\mathbb{E}\|W_n\|^2 \approx \rho^n \mathbb{E}\|W_0\|^2 + \gamma(\rho^n - 1). \quad (52)$$

In the main text, we denote the baseline (divergent) regime by (α, R) , which is the specialization of (γ, ρ) under the empirical fits:

$$R := \rho(s_{\text{new}}, s_{\text{old}}; K), \quad \alpha := \gamma(s_{\text{new}}, b_{\text{new}}, s_{\text{old}}, b_{\text{old}}). \quad (53)$$

Using notations above, Eq. (52) can be rewritten as:

$$\mathbb{E}\|W_n\|^2 \approx R^n \mathbb{E}\|W_0\|^2 + \alpha(R^n - 1), \quad (54)$$

which is exactly Eq. (12). In particular, $R > 1$ indicates an approximately exponential growth trend in $\mathbb{E}\|W_n\|^2$ under the baseline empirical fits. We will introduce an alternative parametrization (β, r) for the NAS (stable) regime in the next subsection.

B.4. Proof for Cor. 3.3

We now analyze our method, which introduces a negative feedback by enforcing a constant target norm for the post-edit value vector. Specifically, we impose

$$\|v_n^{\text{new}}\|^2 := a > 0. \quad (55)$$

Equivalently,

$$\mathbb{E}[\|v_n^{\text{new}}\|^2 \mid W_{n-1}] = a. \quad (56)$$

Using the same linear-fit notation as in Appendix B.3, this corresponds to the specialization

$$s_{\text{new}} = 0, \quad b_{\text{new}} = a. \quad (57)$$

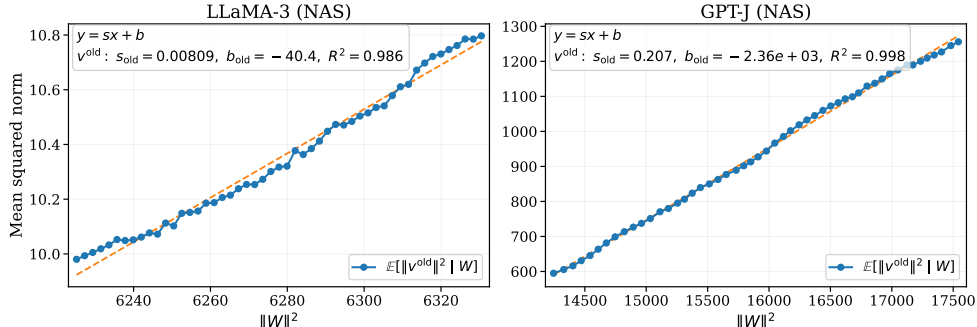


Figure 10. Linear scaling between the pre-edit value norm and the edited weight norm (NAS). Under norm anchoring, we plot $\mathbb{E}[\|v_n^{\text{old}}\|^2 \mid W]$ versus $\|W\|^2$ at multiple checkpoints (averaged over sampled edits/keys). Dashed lines are linear fits; insets report fitted slopes and R^2 .

Meanwhile, within the same observation range (Fig. 10), we empirically find an approximately stable linear scaling for the pre-edit value norm:

$$\mathbb{E}\|v_n^{\text{old}}\|^2 \approx s_{\text{old}} \mathbb{E}\|W_{n-1}\|^2 + b_{\text{old}}. \quad (58)$$

Recall the unified parametrization in Appendix B.3 (Eq. (48)). Under the NAS specialization $s_{\text{new}} = 0$ and $b_{\text{new}} = a$, we have

$$\rho = \rho(0, s_{\text{old}}; K) = 1 - Ks_{\text{old}}, \quad \gamma = \gamma(0, a, s_{\text{old}}, b_{\text{old}}) = \frac{a - b_{\text{old}}}{0 - s_{\text{old}}}. \quad (59)$$

Following the same derivation as in Appendix B.3, substituting $\|v_n^{\text{new}}\|^2 \mapsto a$ and using Eq. (58) yields

$$\mathbb{E}\|W_n\|^2 \approx \rho \mathbb{E}\|W_{n-1}\|^2 + (\rho - 1)\gamma. \quad (60)$$

Solving Eq. (60) gives

$$\mathbb{E}\|W_n\|^2 \approx \rho^n \mathbb{E}\|W_0\|^2 + \gamma(\rho^n - 1). \quad (61)$$

In the main text, we reparametrize the NAS (stable) regime by (β, r) to highlight boundedness:

$$r := \rho(0, s_{\text{old}}; K) = 1 - Ks_{\text{old}}, \quad \beta := -\gamma(0, a, s_{\text{old}}, b_{\text{old}}) = \frac{a - b_{\text{old}}}{s_{\text{old}}}. \quad (62)$$

Substituting Eq. (62) into Eq. (61) yields

$$\mathbb{E}\|W_n\|^2 \approx r^n \mathbb{E}\|W_0\|^2 + \beta(1 - r^n). \quad (63)$$

which is exactly Eq. 16. In our experiments, the fitted slope satisfies $s_{\text{old}} > 0$ and the estimated product Ks_{old} lies in $(0, 1)$ over the observation range, hence $0 < r = 1 - Ks_{\text{old}} < 1$. Moreover, we typically observe $b_{\text{old}} < 0$ and we set $a > 0$, so $\beta = \frac{a - b_{\text{old}}}{s_{\text{old}}} > 0$. Therefore, Eq. (63) suggests that $\mathbb{E}\|W_n\|^2$ remains uniformly bounded over n .

B.5. General Case for $C \neq I$

lemma 3.1 (General C Case). For general C case, Eq. (12) in Lemma 3.1 becomes

$$\|\tilde{W}_n\|^2 = \|\tilde{W}_{n-1}\|^2 + \frac{\|v_n^{\text{new}}\|^2 - \|v_n^{\text{old}}\|^2}{\|\tilde{k}_n\|^2},$$

(64)

where

$$\tilde{W}_n := W_n C^{1/2}, \quad \Delta \tilde{W}_n := \Delta W_n C^{1/2}, \quad \tilde{k}_n := C^{-1/2} k_n^*. \quad (65)$$

Proof: Consider Eq. 10:

$$\Delta W = \frac{(v^{\text{new}} - v^{\text{old}})(C^{-1} k^*)^\top}{k^{*\top} C^{-1} k^*}. \quad (66)$$

For the denominator, note that

$$k^{*\top} C^{-1} k^* = (C^{-1/2} k_n^*)^\top (C^{-1/2} k_n^*) = \tilde{k}_n^\top \tilde{k}_n = \|\tilde{k}_n\|^2. \quad (67)$$

For the numerator, observe that

$$(C^{-1} k_n^*)^\top = (C^{-1/2} (C^{-1/2} k_n^*))^\top = (C^{-1/2} \tilde{k}_n)^\top = \tilde{k}_n^\top (C^{-1/2})^\top = \tilde{k}_n^\top C^{-1/2}. \quad (68)$$

Therefore,

$$\Delta W_n = \frac{(v_n^{\text{new}} - v_n^{\text{old}}) \tilde{k}_n^\top C^{-1/2}}{\|\tilde{k}_n\|^2}. \quad (69)$$

Since $W_n = W_{n-1} + \Delta W_n$, multiplying both sides by $C^{1/2}$ gives

$$\tilde{W}_n = \tilde{W}_{n-1} + \Delta \tilde{W}_n, \quad (70)$$

where

$$\Delta \tilde{W}_n = \Delta W_n C^{1/2} = \frac{(v_n^{\text{new}} - v_n^{\text{old}}) \tilde{k}_n^\top}{\|\tilde{k}_n\|^2}. \quad (71)$$

Eqs. (70) and (71) have the same form as Eqs. (8) and (11) under $C = I$. Thus, by replacing (W_n, k_n^*) with $(\tilde{W}_n, \tilde{k}_n)$ in Appendix B.2, we obtain

$$\|\tilde{W}_n\|^2 = \|\tilde{W}_{n-1}\|^2 + \frac{\|v_n^{\text{new}}\|^2 - \|v_n^{\text{old}}\|^2}{\|\tilde{k}_n\|^2}, \quad (72)$$

which completes the proof.

Propositon 3.2 (General C Case). For general C case, Eq. (3.2) in Prop. 3.2 becomes

$$\boxed{\mathbb{E}\|\tilde{W}_n\|^2 \approx R^n \mathbb{E}\|\tilde{W}_0\|^2 + \alpha(R^n - 1)}, \quad (73)$$

where $R > 1$. The derivation is identical to Appendix B.3, by replacing W_n, k_n^* with the “tilde” versions defined in Eq. (65).

Proof: Recall that the proof of Prop.3.2 directly begins with Eq. (12), which has the same form as Eq. (64) above. Therefore we can very well reuse the derivation in Prop.3.2 line-by-line. The only caveat here is whether the empirical observations in Fig. 8, Fig. 9, still hold under the “tilde” transformation. Concretely, the two approximations used in Appendix B.3 should be replaced by:

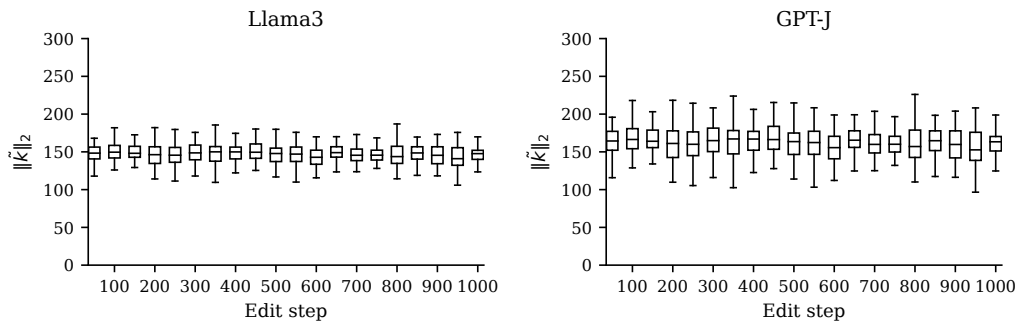


Figure 11. $\|\tilde{k}_n^*\|^2$ stability across edit steps. Boxplots of $\|\tilde{k}_n^*\|$ over edit steps show small fluctuation and tight concentration, supporting the approximation $\|\tilde{k}_n^*\|^{-2} \approx \tilde{K}$ used in the analysis.

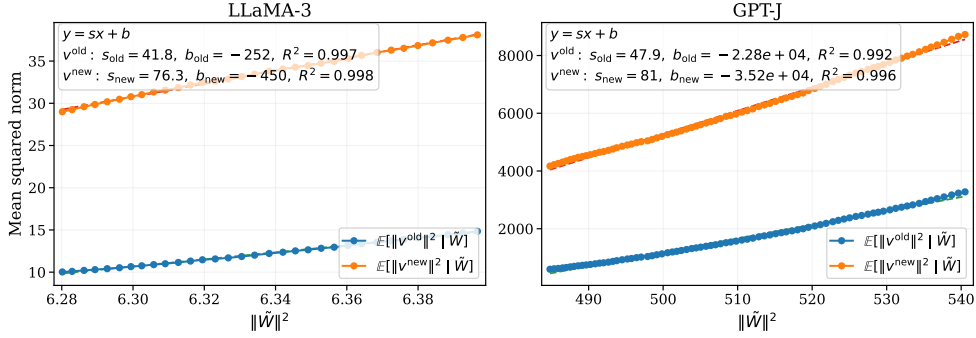


Figure 12. Linear scaling between value-vector norms and the edited weight norm (baseline, tilde space). For sequential editing, we plot $\mathbb{E}[\|v^{\text{new}}\|^2 | \tilde{W}]$ and $\mathbb{E}[\|v^{\text{old}}\|^2 | \tilde{W}]$ versus $\|\tilde{W}\|^2$ at multiple checkpoints (averaged over sampled edits/keys). Dashed lines are linear fits; insets report fitted slopes and R^2 . The fitted slope for v^{new} is consistently larger than that for v^{old} .

1. $\|\tilde{k}_n\|^2$ Stability (Fig. 11). Replace

$$\|k_n^*\|^{-2} \approx K$$

by

$$\|\tilde{k}_n\|^{-2} \approx \tilde{K},$$

i.e., $\|\tilde{k}_n\|^{-2}$ remains stable around a constant during sequential edits.

2. Linear fits (Fig. 12). Replace

$$\mathbb{E}[\|v_n^{\text{new}}\|^2 | \|W_{n-1}\|^2] \approx s_{\text{new}}\|W_{n-1}\|^2 + b_{\text{new}}, \quad \mathbb{E}[\|v_n^{\text{old}}\|^2 | \|W_{n-1}\|^2] \approx s_{\text{old}}\|W_{n-1}\|^2 + b_{\text{old}}$$

by the corresponding relations for the “tilde” versions:

$$\mathbb{E}[\|v_n^{\text{new}}\|^2 | \|\tilde{W}_{n-1}\|^2] \approx s_{\text{new}}\|\tilde{W}_{n-1}\|^2 + b_{\text{new}}, \quad \mathbb{E}[\|v_n^{\text{old}}\|^2 | \|\tilde{W}_{n-1}\|^2] \approx s_{\text{old}}\|\tilde{W}_{n-1}\|^2 + b_{\text{old}}.$$

Under these empirical observations for the “tilde” versions, we can define (α, R) (resp. (β, r)) for the general C case. And the derivation in Appendix B.3 can be reused line-by-line, yielding Eq. (73).

Corollary 3.3 (General C Case). For general C case, Eq. (3.3) in Prop. 3.3 becomes

$$\boxed{\mathbb{E}\|\tilde{W}_n\|^2 \approx r^n \mathbb{E}\|\tilde{W}_0\|^2 + \beta(1 - r^n)}, \quad (74)$$

where $\beta > 0$, $r \in (0, 1)$.

Proof: Similar to **Proposition 3.2 (General C Case)**, to reuse the derivation in Appendix B.4, it suffices to verify that the after-NAS empirical fit used in Appendix B.4 remains valid under the transformation in Eq. (65). Specifically, the approximately stable relation in the observation range,

$$\mathbb{E}\|v_n^{\text{old}}\|^2 \approx s_{\text{old}}\mathbb{E}\|W_{n-1}\|^2 + b_{\text{old}},$$

should be replaced in the general C case by: (Fig. 13)

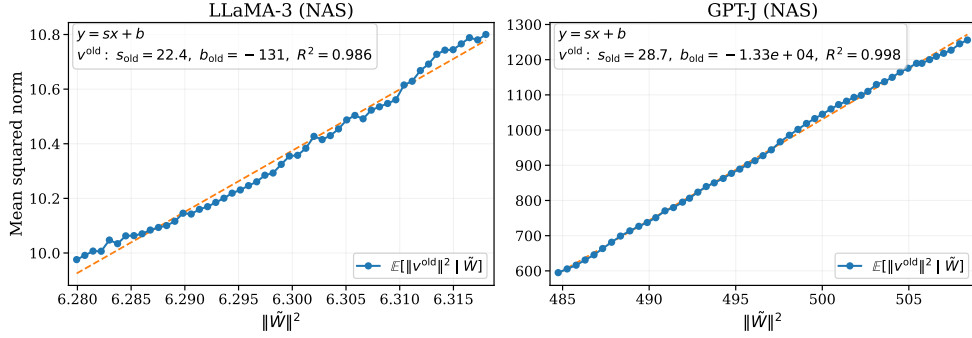


Figure 13. Linear scaling between the pre-edit value norm and the edited weight norm (NAS, tilde space). Under norm anchoring, we plot $\mathbb{E}[\|v_n^{\text{old}}\|^2 | \tilde{W}]$ versus $\|\tilde{W}\|^2$ at multiple checkpoints (averaged over sampled edits/keys). Dashed lines are linear fits; insets report fitted slopes and R^2 .

$$\mathbb{E}\|v_n^{\text{old}}\|^2 \approx s_{\text{old}} \mathbb{E}\|\tilde{W}_{n-1}\|^2 + b_{\text{old}}.$$

Since the above ‘‘tilde’’ empirical phenomenon also holds, the remaining computations in Appendix B.4 can be reused line-by-line, yielding the corresponding conclusion of Cor. 3.3 for the general C case.

C. Additional Experiment

C.1. Additional General Capability Experiment

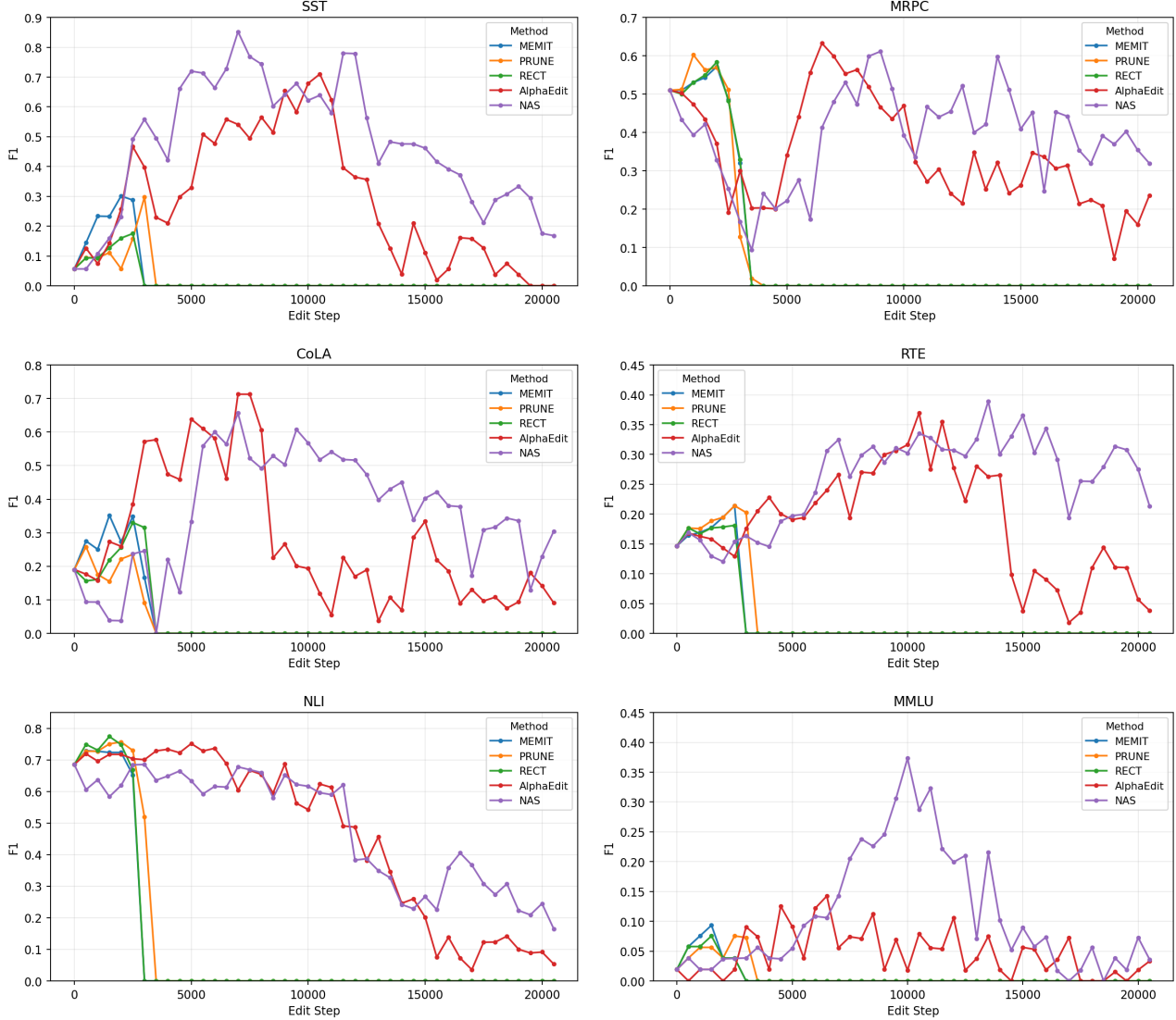


Figure 14. GLUE F1 trajectories over sequential edits on Qwen (step 0 denotes the pre-edit baseline).

C.1.1. QWEN2.5

Appendix Fig. 14 reports the evolution of GLUE F1 on Qwen as the number of edits increases (step 0 is the pre-edit baseline). Across all six tasks, NAS yields consistently stronger retention of general language understanding compared with prior locate-and-edit editors, with the gap becoming most visible in the long-horizon regime where cumulative interference typically dominates. This behavior supports our central claim that NAS acts as a plug-in stabilizer for lifelong knowledge updating: by controlling the destabilizing drift induced by repeated localized rewrites, it substantially reduces collateral degradation on out-of-distribution evaluation suites such as GLUE.

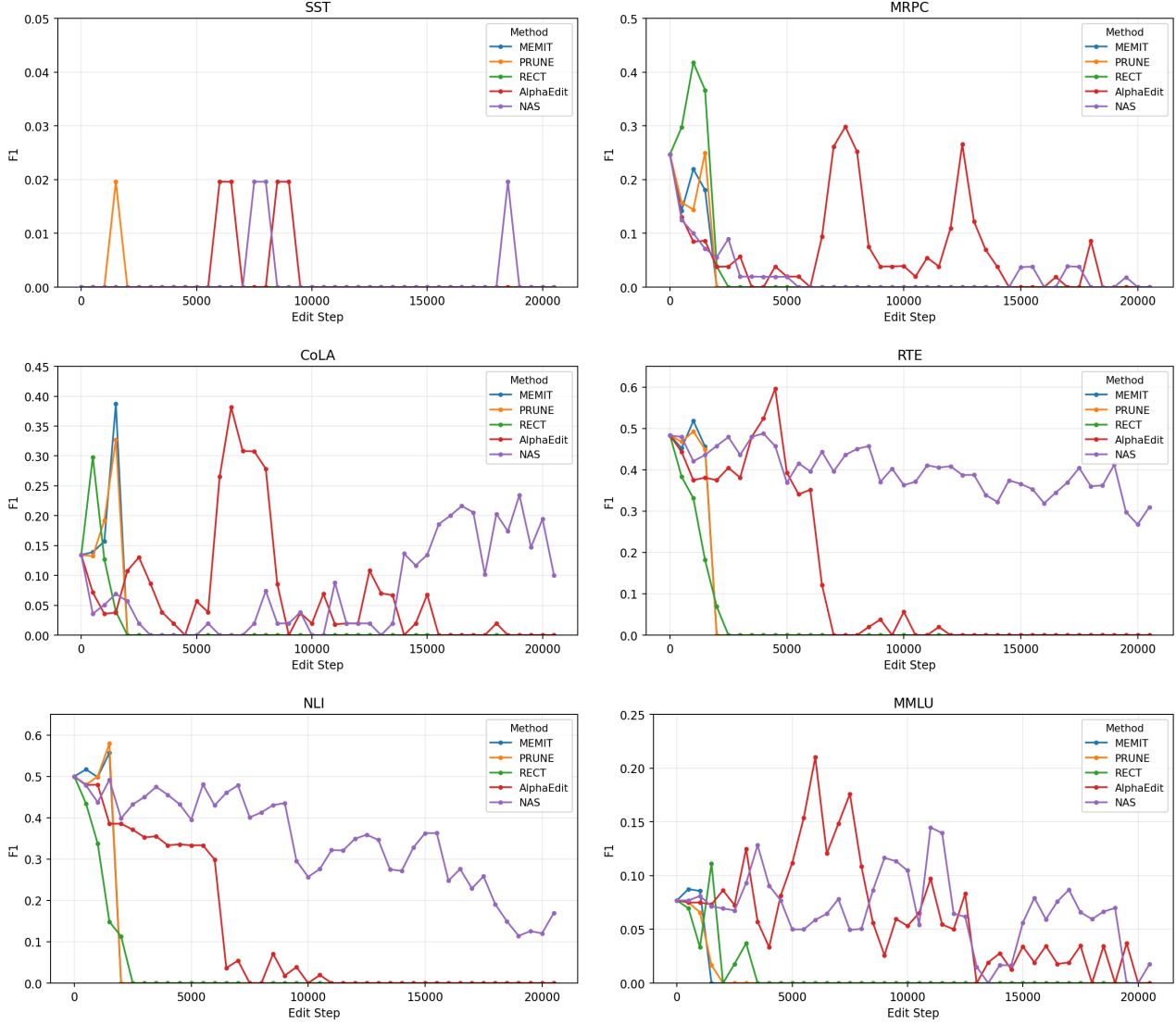


Figure 15. GLUE F1 trajectories over sequential edits on GPT-J (step 0 denotes the pre-edit baseline).

C.1.2. GPT-J

A similar trend is observed on GPT-J in Appendix Fig. 15, where the backbone is generally more fragile under repeated edits. Despite the lower absolute starting performance on some tasks, NAS markedly improves long-horizon stability, maintaining non-trivial GLUE performance in stages where competing editors often exhibit sharp degradation. The fact that the same plug-in provides clear benefits on both Qwen and GPT-J indicates that NAS captures a model-agnostic stabilization effect, rather than exploiting idiosyncrasies of a specific backbone or task, reinforcing its practicality for sequential deployment.

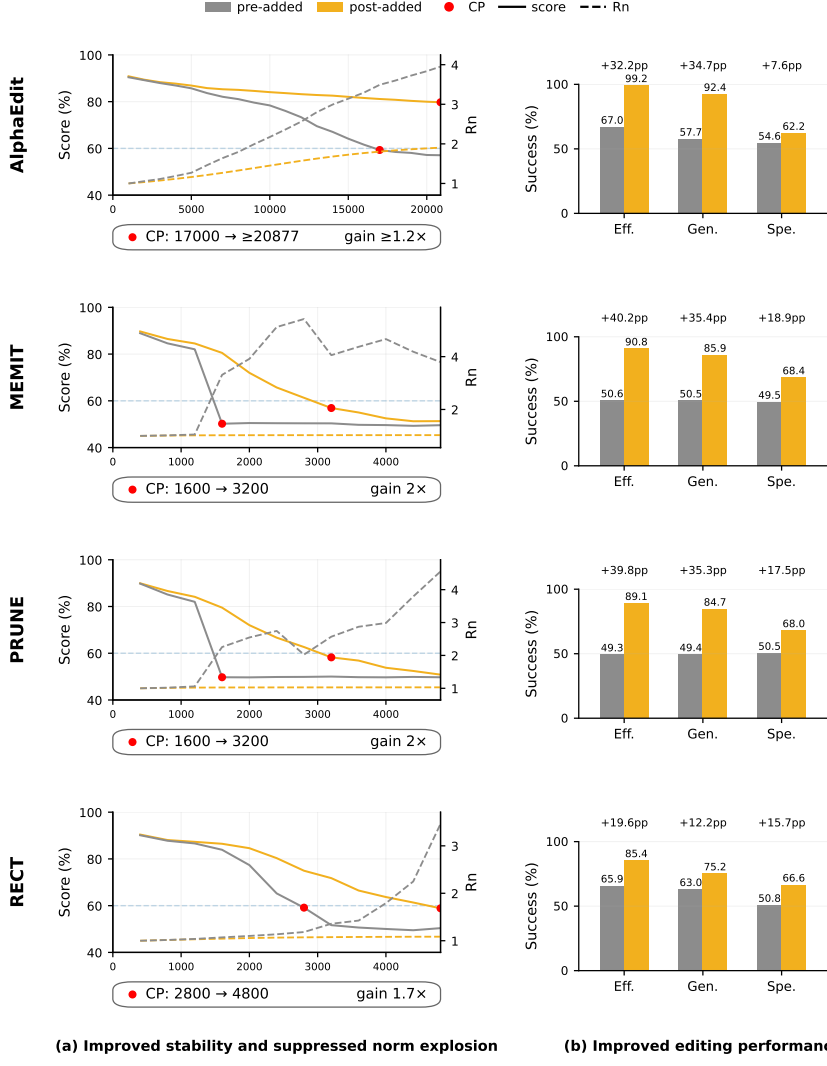


Figure 16. NAS improves stability and editing performance on GPT-J. (a) Improved stability and suppressed norm explosion: dual-axis trajectories show the editing score (solid) and relative weight norm R_n (dashed); the red dot marks the collapse point (CP, first step with score ≤ 60). (b) Improved editing performance: success at the original (w/o NAS) CP, reported on rewrite/para./neighbor (Eff./Gen./Spe.), comparing pre-added vs. post-added.

C.2. Plug in Experiment on GPT-J.

We further validate the plug-in behavior of NAS on an additional backbone, GPT-J, using the same experimental setup as in the main text. We integrate NAS into four representative Locate-and-Edit editors (MEMIT, PRUNE, RECT, and AlphaEdit) and run long-horizon sequential editing on CounterFact, tracking both the editing score and the relative weight-norm statistic R_n .

Figure 16 summarizes the results. Across all four editors, attaching NAS reliably suppresses the growth of R_n and delays the collapse point (CP), indicating that the stabilization effect is not specific to Llama3-8B. In particular, NAS extends the editable horizon by $2 \times$ for MEMIT and PRUNE (CP: 1600 → 3200), by $1.7 \times$ for RECT (2800 → 4800), and by at least $1.2 \times$ for AlphaEdit ($17,000 \rightarrow \geq 20,877$), where the NAS-augmented run does not collapse within the full CounterFact stream.

In addition to improved stability, NAS also improves editing quality under a shared reference condition. Evaluated at the original (w/o NAS) CP of each base editor, NAS substantially increases post-edit success on rewrite/paraphrase/neighborhood (Eff./Gen./Spe.) across methods. The gains are large and consistent, with typical improvements of roughly $+20\text{--}+40$

percentage points on efficacy and generalization, and $+8\text{--}19$ percentage points on specificity, mirroring the main-paper findings. Overall, the GPT-J results corroborate that NAS is a portable, plug-and-play stabilization component that both mitigates instability (via suppressing norm growth) and improves editing performance across diverse L&E baselines.

C.3. Results on Additional Base Models

Table 3. Additional Long-Horizon Sequential model editing results on GPT2-XL. Pre-edited is separated by a rule; Best in **bold**, second-best in underlined.

Model	Method	Counterfact					ZsRE		
		Eff. \uparrow	Gen. \uparrow	Spe. \uparrow	Flu. \uparrow	Consis. \uparrow	Eff. \uparrow	Gen. \uparrow	Spe. \uparrow
GPT2-XL	Pre-edited	21.34 ± 0.25	24.07 ± 0.31	78.72 ± 0.19	527.26 ± 0.88	2.86 ± 0.04	22.59 ± 0.22	21.80 ± 0.18	24.33 ± 0.21
	MEMIT	49.56 ± 0.14	49.56 ± 0.14	50.42 ± 0.22	496.38 ± 0.45	4.34 ± 0.11	0.00 ± 0.00	0.00 ± 0.00	0.00 ± 0.00
	PRUNE	47.86 ± 0.21	48.14 ± 0.19	52.72 ± 0.25	469.10 ± 0.72	4.32 ± 0.13	0.00 ± 0.00	0.00 ± 0.00	0.00 ± 0.00
	RECT	47.66 ± 0.18	47.47 ± 0.23	52.32 ± 0.29	235.52 ± 0.33	0.70 ± 0.02	0.00 ± 0.00	0.00 ± 0.00	0.00 ± 0.00
	AlphaEdit	73.92 ± 0.28	58.16 ± 0.24	54.20 ± 0.31	566.62 ± 1.02	14.53 ± 0.27	43.62 ± 0.33	35.90 ± 0.29	10.52 ± 0.11
	NAS	91.72 ± 0.18	73.15 ± 0.25	56.76 ± 0.22	568.23 ± 0.95	27.97 ± 0.31	58.54 ± 0.26	49.32 ± 0.28	12.76 ± 0.15

We further evaluate Locate-and-Edit (L&E) editors on **GPT2-XL** under the **same sequential editing setup as RQ1**. Table 3 reports the long-horizon sequential editing results. Consistent with our main findings, several L&E baselines exhibit severe degradation on ZsRE, collapsing to **0** post-edit success for MEMIT/PRUNE/RECT. ALPHAEDIT remains substantially more stable, and NAS achieves the best performance across *all* reported metrics on both CounterFact and ZsRE. In particular, NAS improves over ALPHAEDIT by **+17.8/+15.0/+2.6** points on CounterFact (Eff./Gen./Spe.) and **+14.9/+13.4/+2.2** on ZsRE, while also markedly increasing consistency (**+13.4**). These results further support the robustness and portability of NAS to additional backbones beyond those in the main text.

C.4. Additional Baselines under Official Sequential-Editing Configurations

Motivation and protocol. To complement the main results, we report additional baselines that are not included in the main tables due to *protocol mismatch*: several non-L&E editors do not support our *atomic sequential editing* setting (i.e., updating exactly one fact per step), and are instead designed and tuned for their own official update granularity and step sizes. To avoid redefining these methods, we evaluate all additional baselines using their *official* sequential-editing configurations and learning-rate/step schedules. MEMOIR does not support our generation-based evaluation, hence Fluency/Consistency entries are marked as NULL.

NAS under two sequential-editing granularities. For a controlled comparison against these official settings, we report two variants of our method: NAS follows the atomic protocol used throughout the paper, whereas NAS^\dagger follows the batched sequential-editing configuration (updating 500 facts per update step) to match the granularity used by several additional baselines. Tab. 4 summarizes results after 10,000 sequential edits.

Summary. Across additional baselines and backbones, NAS consistently achieves a favorable efficacy–generalization balance under sequential editing, while several methods exhibit strong efficacy/locality but weak generalization. We highlight two representative cases below.

Observations. Tab. 4 suggests that additional baselines can score highly on efficacy/locality while failing to generalize. On LLaMA3/CounterFact, GRACE reaches Eff./Spe.=99.08/88.39 (with Flu.=630.42), but its Gen. is 10.20; on LLaMA3/ZsRE, its Gen. further drops to 1.84. In contrast, NAS yields a more balanced profile on the same backbone: on CounterFact, NAS achieves Eff./Gen./Spe.=98.85/85.50/64.62 and NAS^\dagger achieves 98.64/88.21/66.13; on ZsRE, NAS attains Eff./Gen.=92.76/88.71 and NAS^\dagger attains 93.74/89.39.

Example: GPT-J. On GPT-J, NAS improves efficacy and generalization simultaneously. On CounterFact, NAS and NAS^\dagger achieve Eff./Gen.=99.60/93.36 and 99.61/93.92, respectively, compared to GRACE (Gen.=16.40) and WISE (Gen.=43.02). LyapLock attains high specificity (Spe.=83.05) but with substantially lower Eff./Gen. (47.56/34.60). On ZsRE, NAS^\dagger achieves Eff./Gen.=97.65/92.78, compared to LyapLock 64.23/58.62.

Table 4. Sequential model editing results on additional baselines (10,000 sequential edits). Rows are visually grouped by whether the method belongs to the L&E family; *best/second* are computed across *all* methods within each backbone (ignoring NULL entries). Best in **bold**, second-best in underlined.

Model	Method	Counterfact					ZsRE		
		Eff. \uparrow	Gen. \uparrow	Spe. \uparrow	Flu. \uparrow	Consis. \uparrow	Eff. \uparrow	Gen. \uparrow	Spe. \uparrow
LLaMA3	GRACE	99.08	10.20	88.39	630.42	24.40	90.16	1.84	17.52
	WISE	17.90	20.23	<u>80.79</u>	355.55	1.63	31.77	31.26	24.59
	MEMOIR	90.44	64.84	<u>54.71</u>	NULL	NULL	90.15	87.67	31.78
	ENCORE	92.03	84.44	56.98	577.27	26.81	90.86	87.31	31.51
	LyapLock	37.40	26.96	70.38	601.12	27.32	77.09	72.22	28.90
	NAS	<u>98.85</u>	<u>85.50</u>	64.62	619.99	<u>29.93</u>	92.76	<u>88.71</u>	32.28
	NAS †	98.64	88.21	<u>66.13</u>	<u>625.07</u>	31.35	93.74	89.39	<u>32.18</u>
Qwen2.5	GRACE	96.05	16.49	84.48	334.05	6.44	98.64	0.85	20.04
	WISE	11.76	36.45	<u>83.94</u>	397.35	3.80	30.91	32.43	<u>25.87</u>
	NAS	<u>98.22</u>	<u>65.48</u>	76.42	<u>621.36</u>	<u>29.83</u>	72.15	<u>60.09</u>	18.78
	NAS †	99.21	77.21	74.86	<u>621.37</u>	31.76	<u>98.48</u>	91.00	44.68
GPT-J	GRACE	99.27	16.40	<u>80.81</u>	621.62	29.78	<u>93.77</u>	1.62	17.99
	MEMOIR	87.56	49.93	52.45	NULL	NULL	84.19	78.56	<u>27.23</u>
	WISE	45.85	43.02	58.33	510.89	8.80	32.73	29.08	26.00
	LyapLock	47.56	34.60	83.05	591.39	30.82	64.23	58.62	29.25
	NAS	<u>99.60</u>	<u>93.36</u>	67.00	<u>611.39</u>	<u>39.57</u>	92.74	<u>81.28</u>	24.32
	NAS †	99.61	93.92	67.19	609.90	42.25	97.65	92.78	24.60
GPT2-XL	GRACE	99.14	16.92	77.18	526.09	3.03	<u>92.73</u>	1.39	25.15
	MELO	61.48	47.15	53.92	542.73	11.63	68.15	69.65	19.56
	WISE	33.12	33.48	67.27	541.08	6.20	37.52	39.23	<u>40.27</u>
	ENCORE	92.92	77.09	57.79	514.90	23.40	86.40	<u>77.33</u>	24.66
	LyapLock	31.80	28.68	<u>76.81</u>	621.09	31.29	34.76	32.73	25.82
GPT2-XL	NAS	96.98	<u>82.03</u>	59.24	557.40	<u>33.18</u>	72.38	64.64	16.93
	NAS †	<u>97.24</u>	83.77	59.54	<u>566.36</u>	35.32	97.07	87.74	43.18

Transition. To further assess the additional editors of the L&E-paradigm and the effect of enabling NAS as a plug-in, we turn to a longer-horizon evaluation of WikiBigEdit in the next section.

C.5. Plug-in Experiments of Additional L&E methods on WikiBigEdit

Setup. We evaluate long-horizon *atomic sequential editing* on WikiBigEdit, where each edit updates exactly one fact before proceeding to the next. We periodically evaluate at increasing checkpoints up to 32,541 edits. We report Efficacy (ES), Generalization (GS), and Specificity (LS), and summarize them using Score = (ES + GS + LS)/3.

Additional plug-in results. We further enable NAS as a *drop-in* component for existing LE editors by toggling a single additional line of code while keeping other hyperparameters and settings unchanged. Fig. 17 compares ENCORE and LyapLock with vs. without NAS. ENCORE without NAS collapses around ~ 25 k edits and degrades to near-zero accuracy thereafter, whereas ENCORE+NAS remains stable through the full horizon. Concretely, at 32,541 edits ENCORE improves from ES/GS/LS = 4.77/3.80/2.92 (Score 3.83) to 76.83/67.75/45.91 (Score 63.50) with NAS (Tab. 5). Similarly, NAS consistently improves LyapLock across checkpoints, yielding ES/GS/LS = 75.72/64.13/41.75 (Score 60.53) at 32,541 edits, compared to 62.60/55.10/29.24 (Score 48.98) without NAS.

Reference performance of NAS. For reference, we also report results of NAS under the same setting. At 32,541 edits, NAS attains ES/GS/LS = 80.45/68.74/43.17 (Score 64.12) (Tab. 5).

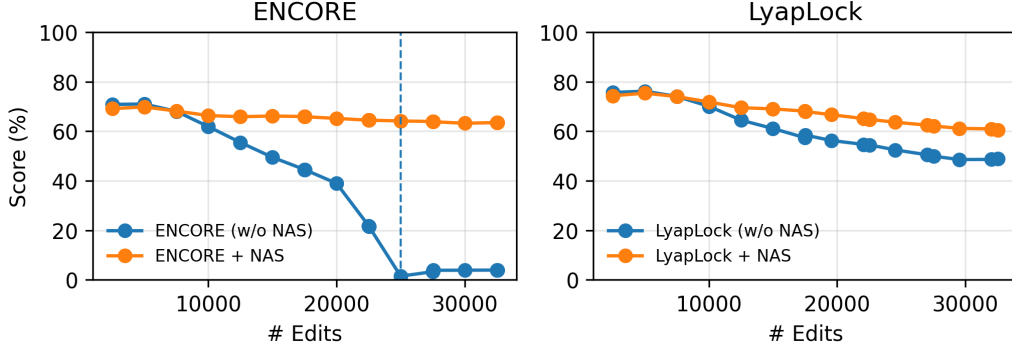


Figure 17. Single-step sequential editing on WikiBigEdit: ENCORE and LyapLock with vs. without NAS (Score = (ES + GS + LS)/3).

Table 5. Single-step sequential editing on WikiBigEdit at 32,541 edits (%; higher is better).

Method	ES	GS	LS	Score
ENCORE	4.77	3.80	2.92	3.83
ENCORE + NAS	76.83	67.75	45.91	63.50
LyapLock	62.60	55.10	29.24	48.98
LyapLock + NAS	75.72	64.13	41.75	60.53
NAS	80.45	68.74	43.17	64.12

Takeaway. Overall, NAS serves as a simple and effective plug-in that substantially improves long-horizon stability under single-step sequential editing when combined with prior LE methods.

C.6. Runtime Overhead of Norm-Anchor Scaling (NAS)

We compare the wall-clock runtime with and without NAS under identical editing hyperparameters. Following our sequential-editing setup on **Llama3-8B**, we run $n=100$ edits for each method and report the per-edit runtime (mean \pm std). We summarize the relative overhead as $\Delta\% = \frac{t_{\text{NAS}} - t_{\text{base}}}{t_{\text{base}}} \times 100\%$.

Table 6. Runtime comparison with/without NAS. We report mean \pm std seconds per edit over $n=100$ edits. $\Delta\%$ is computed on the per-edit mean runtime.

Method	w/o NAS (s/edit)	w/ NAS (s/edit)	$\Delta\%$
MEMIT	5.20 ± 0.82	5.20 ± 0.68	+0.00
PRUNE	5.17 ± 0.62	5.18 ± 0.68	+0.19
RECT	8.18 ± 0.84	8.08 ± 0.78	-1.22
AlphaEdit	6.75 ± 0.73	6.78 ± 0.79	+0.44

Overall, enabling NAS introduces negligible runtime overhead. Across all tested editors, the per-edit runtime change remains within $\pm 1.3\%$, and is typically below 0.5%. Given that NAS only adds lightweight vector re-scaling (without extra optimization steps), the observed differences are well within the natural variance of per-edit runtime (see the reported std values), supporting that NAS is effectively runtime-free in practice.

D. Examples of CounterFact and ZsRE dataset

D.1. CounterFact Examples

1. Twin-city relation (P190).

- **Subject:** Lyon

- **Prompt template:** What is the twin city of {}? It is
- **Target (true → new):** Beirut → Manila
- **Context / paraphrase prompts (examples):**
 - Lyon is a twin city of
 - The twin city of Lyon is
- **Locality prompts (same relation; other subjects, examples):**
 - What is the twin city of Los Angeles? It is
 - Athens is a twin city of
 - The twin city of Beijing is
- **Neighborhood prompts (subject-related, examples):**
 - Lyon's twin city is known for
 - People in Lyon's twin city speak the language of

2. Mother-tongue relation (P103).

- **Subject:** Thomas Joannes Stieltjes
- **Prompt template:** The mother tongue of {} is
- **Target (true → new):** Dutch → English
- **Context / paraphrase prompts (examples):**
 - Thomas Joannes Stieltjes spoke the language
 - Thomas Joannes Stieltjes, speaker of
- **Locality prompts (same relation; other subjects, examples):**
 - The mother tongue of Rob Birza is
 - Arend Lijphart is a native speaker of
 - The native language of Charlie Chaplin is

3. Citizenship relation (P27).

- **Subject:** Mahmoud Fawzi
- **Prompt template:** {} has a citizenship from
- **Target (true → new):** Egypt → Germany
- **Context / paraphrase prompts (examples):**
 - Mahmoud Fawzi holds a citizenship from
 - Mahmoud Fawzi, who is a citizen of
- **Locality prompts (same relation; other subjects, examples):**
 - Imhotep, who is a citizen of
 - Marc Forster holds a citizenship from
 - Katja Ebstein, who is a citizen of

D.2. ZsRE Examples

1. Publisher query.

- **Subject:** Alien Front Online
- **Prompt:** What company published Alien Front Online?
- **Target (true → new):** Sega → 2K Games
- **Rephrase prompt:** Which company released Alien Front Online?
- **Locality (Relation.Specifity, examples):**
 - The country of origin of Alien Front Online is → Japan
 - Alien Front Online country of origin → Japan
- **Portability (Reasoning, example):**

- Who is the parent company of the publisher of Alien Front Online? → Take-Two Interactive

2. Programming-language query.

- **Subject:** GNOME Chess
- **Prompt:** What programming language was used to write GNOME Chess?
- **Target (true → new):** Vala → Python
- **Rephrase prompt:** How is the programming language for GNOME Chess?
- **Locality (Relation_Specificity, examples):**
 - The platform of GNOME Chess is → Unix-like operating system
 - GNOME Chess platform → Unix-like operating system
- **Portability (Reasoning, example):**
 - Who created the programming language used to write GNOME Chess? → Guido van Rossum

3. Launch-year query.

- **Subject:** Old Quebec Street Mall
- **Prompt:** When was Old Quebec Street Mall launched?
- **Target (true → new):** 2003 → 2002
- **Rephrase prompt:** When did Old Quebec Street Mall open?
- **Locality (Relation_Specificity, examples):**
 - The located in the administrative territorial entity of Old Quebec Street Mall is → Guelph
 - Old Quebec Street Mall located in the administrative territorial entity → Guelph
- **Portability (Reasoning, example):**
 - What major sporting event took place the same year Old Quebec Street Mall was launched? → Salt Lake City Winter Olympics